

Erlend Randen

# Condition monitoring - Validation of flowmeters

Master's thesis in Mechanical Engineering

Supervisor: Lars Eirik Bakken

Co-supervisor: Erik Langørgen

June 2021



Erlend Randen

# **Condition monitoring - Validation of flowmeters**

Master's thesis in Mechanical Engineering  
Supervisor: Lars Eirik Bakken  
Co-supervisor: Erik Langørgen  
June 2021

Norwegian University of Science and Technology  
Faculty of Engineering  
Department of Energy and Process Engineering





## Acknowledgements

This master thesis is a part of the Master of Science program in the Department of Energy and Process Engineering at the Norwegian University of Science and Technology (NTNU). The master thesis was written during the spring semester of 2021. The workload of the thesis should represent 30 ETCS credits.

I want to thank supervisor Lars Eirik Bakken for guidance and facilitation. His office door has always been open, even in this covid-19 pandemic, whenever there was a need for discussion and evaluation of the thesis. A special thanks to co-supervisor Erik Langørgen for his expertise related to the compressor test facility instrumentation and his responsibility to attend during experiments.

Trondheim, 11-06-2021

Erlend Randen

Erlend Randen



## Abstract

Centrifugal compressors are one of the most important turbomachines utilized and play a fundamental role in the existing world energy situation. Due to the enormous amount of power associated with their industrial applications, even short downtime results in substantial financial losses. Thus, high demands are placed on manufacturers and operators concerning operational reliability. A critical problem that can create downtime is a phenomenon named surge.

*Surge* is an unsteady flow phenomenon occurring at low inlet flow rates. As the compressor is operating under surge condition, the pressure fluctuates cyclically through the compressor. In the worst case, mechanical breakdown occurs. Because of these dangers in operation, surge prediction is crucial, which requires reliable process data. This is especially relevant for the compressor inlet volume flow. Hence, knowledge regarding flow measurement is pivotal when investigating the surge cycle in terms of accuracy, transient, and reverse flow.

The main objective of the work has been to contribute to the investigation of surge cycle research in the Norwegian University of Science and Technology (NTNU) compressor test facility related to reliable flow measurements. An uncertainty analysis and pressure test has been performed to investigate if the existing flowmeters give an accurate and reliable measurement under the surge cycle.

The applied uncertainty analysis shows a relative expanded uncertainty of over 5 % with a mass flow rate under 0.5 kg/s on the compressor test facility orifice plate. The pressure test shows a slow response time and a signal delay of 160 ms between the orifice plate and venturi meter. Based on an overall assessment, new differential pressure transmitters were acquired to improve the accuracy at low flow rates, give a faster response time and remove the signal delay.

Further, how reverse flow affects the venturi meter is vital in the investigation of the surge cycle. An experimental test has been conducted using a reliable orifice plate as a reference to see how reverse flow affects the venturi meter. The experimental result reveals that the venturi meter gives a significant measuring error under reverse flow compared to normal flow. In addition, a compressor surge cycle experiment has been explored. A negative DP value was detected on the venturi meter, which of the principle of fluid mechanics should not occur and calls for further investigations.





## Abstract in Norwegian

Sentrifugalkompressor er en av de viktigste turbomaskinene som brukes og spiller en sentral rolle i den nåværende energi situasjonen. På grunn av den enorme mengden effekt assosiert med de industrielle applikasjonene vil selv korte stopp resultere i vesentlig finansielle tap. Dermed stilles høye krav til produsent og operatør i forhold til operasjonell pålitelighet. Et kritisk problem som kan generere stopp er et fenomen kalt surge.

*Surge* er et ustabilisert strømnings fenomen som opptrer ved lave innløps strømninger. Når kompressoren operer i surge vil trykket fluktuere syklisk gjennom kompressoren og i ytterste konsekvens oppstår mekanisk sammenbrudd. På grunn av farene dette medfører er det å kunne forutse surge veldig viktig, noe som krever pålitelige prosessmålinger. Dette er spesielt relevant for målinger av volum strømninger ved kompressorens innløp. Derfor er kunnskap angående strømningsmålinger grunnleggende for å kunne undersøke surge syklus i form av nøyaktighet, pulserende og reverserende strømnings.

Hovedmålet med denne oppgaven har vært å bidra i undersøkelsen av surge syklus ved kompressor anlegget hos Norges Teknisk-Naturvitenskapelige Universitet (NTNU) relatert til pålitelige strømningsmålinger. En usikkerhetsanalyse og trykktest har blitt gjennomført for å undersøke om de eksisterende gjennomstrømningsmålerne gir nøyaktige og pålitelige målinger under surge.

Den anvendte usikkerhetsanalysen viser en relativ utvidet usikkerhet på over 5 % med en massestrøm på under 0.5 kg/s på kompressor anleggets blendeplate. Trykktesten viser en langsom responstid og en signalforsinkelse på 160 ms mellom blendeplaten og venturimeteret. Basert på en helhetsvurdering er nye differensial trykktransmittere anskaffet for å øke nøyaktigheten ved lave strømninger, gi raskere respons tid og fjerne signalforsinkelsen.

Hvordan reverserende strømnings påvirker venturimeter målingene er avgjørende for undersøkelsen av surge syklus. En eksperimentell undersøkelse er gjennomført med bruk av en pålitelig måleblende som referanse for å se hvordan reverserende strømnings påvirker venturimeteret. Testen viser at venturimeteret måler vesentlig feil under reverserende strømnings sammenlignet med normal strømningsretning. I tillegg er et forsøk med kompressor surge syklus undersøkt. Et negativ differensial trykk ble oppdaget på venturimeteret som ifølge fluidmekanikkens lover ikke skal inntreffe og dette må undersøkes nærmere.



# Contents

<b>Acknowledgements</b>	<b>i</b>
<b>Abstract</b>	<b>iii</b>
<b>Abstract in Norwegian</b>	<b>v</b>
<b>Contents</b>	<b>vii</b>
<b>List of Figures</b>	<b>ix</b>
<b>List of Tables</b>	<b>x</b>
<b>Nomenclature</b>	<b>xi</b>
<b>1 Introduction</b>	<b>1</b>
1.1 Background .....	1
1.2 Scope of work.....	2
1.3 Thesis structure.....	3
<b>2 Centrifugal compressor</b>	<b>4</b>
2.1 Principle.....	4
2.2 Compressor thermodynamics.....	4
2.2.1 Performance analysis .....	5
2.3 Performance characteristic.....	6
2.4 Compressor system.....	6
2.5 Surge .....	7
2.6 Summary and conclusion .....	8
<b>3 Differential pressure meter</b>	<b>9</b>
3.1 Principle.....	9
3.2 Orifice plate.....	10
3.3 Venturi tube .....	10
3.4 Reverse flow in differential pressure meters.....	10
3.5 Differential pressure transmitter .....	11
3.6 Summary and conclusion .....	12
<b>4 NTNU Wet gas compressor test facility</b>	<b>13</b>
4.1 Compressor test facility .....	13
4.2 Orifice plate.....	14
4.2.1 Flow calculation ISO 5167-2.....	15
4.2.2 Steady-state and pulsating flow.....	16
4.3 Venturi tube .....	17
4.3.1 Flow calculation ISO 5167-4.....	17
4.4 Instrumentation data .....	18
4.5 Risk assessment .....	19
4.6 Summary and conclusion .....	19

<b>5</b>	<b>Uncertainty and sensitivity analysis</b>	<b>20</b>
5.1	Uncertainty analysis.....	21
5.1.1	Type B evaluation.....	22
5.2	Orifice uncertainty analysis.....	24
5.2.1	Differential pressure transmitter.....	25
5.2.2	Density.....	28
5.2.3	Diameter ratio.....	32
5.2.4	Expansibility factor.....	33
5.2.5	Discharge coefficient.....	34
5.3	Orifice uncertainty analysis result.....	35
5.4	Sensitivity analysis results.....	36
5.5	Recommendation to improve the uncertainty.....	37
<b>6</b>	<b>Experimental results and analysis</b>	<b>40</b>
6.1	Pressure test.....	40
6.2	New test facility setup.....	42
6.3	Validation of venturi meter.....	44
6.4	Surge case.....	48
<b>7</b>	<b>Conclusion and recommendations for further work</b>	<b>51</b>
7.1	Conclusion.....	51
7.2	Recommendations for further work.....	52
<b>8</b>	<b>References</b>	<b>53</b>
<b>9</b>	<b>Appendix</b>	<b>55</b>
<b>A</b>	<b>Risk assessment</b>	<b>i</b>
<b>B</b>	<b>Datasheets</b>	<b>ii</b>
B.1	LD300 D-2.....	ii
B.2	PCE-28.....	iii
B.3	CTP5000/CTR5000.....	iv
B.4	LD300 D-1 and LD300 D-0.....	v
B.5	Protran PR3202.....	vi
B.6	Orifice plate $\beta = 0.6401$ .....	vii
B.7	Orifice plate $\beta = 0.4018$ .....	viii
<b>C</b>	<b>Sensitivity coefficients</b>	<b>ix</b>
<b>D</b>	<b>Uncertainty analysis</b>	<b>x</b>
D.1	LD300 D-1.....	x
D.2	LD300 D-0.....	xi
D.3	Protran PR3202.....	xii

# List of Figures

- 1. The surge cycle ..... 1
- 2. Centrifugal compressor ..... 4
- 3. Compression process ..... 5
- 4. Performance map NTNU's centrifugal compressor [3] ..... 6
- 5. PFD NTNU compressor test facility ..... 6
- 6. Compressor system ..... 7
- 7. The surge cycle ..... 8
- 8. Flow illustration ..... 9
- 9. Venturi tube ..... 10
- 10. DP - Flow relation ..... 11
- 11. Response time ..... 11
- 12. Damping ..... 11
- 13. Resolution ..... 12
- 14. PI&D of relevant equipment at compressor test facility ..... 13
- 15. Test facility orifice plate ..... 14
- 16. Orifice plate mass flow rate iteration ..... 16
- 17. Test facility venturi meter ..... 17
- 18. Type B evaluation ..... 23
- 19. Orifice plate relative expanded uncertainty ..... 35
- 20. Orifice plate sensitivity analysis result with high mass flow rate ..... 36
- 21. Orifice plate sensitivity analysis result with low mass flow rate ..... 36
- 22. Orifice plate relative expanded uncertainty with different plates ..... 37
- 23. Orifice plate relative expanded uncertainty with different DP transmitters ..... 38
- 24. Orifice plate relative expanded uncertainty with longer inlet pipe section ..... 38
- 25. Pressure test setup ..... 40
- 26. Signal delay ..... 40
- 27. Signal correction ..... 40
- 28. Orifice plate relative expanded uncertainty for current and new setup ..... 43
- 29. Steady-state venturi meter validation under normal flow ..... 44
- 30. Steady-state venturi meter validation under reverse flow ..... 45
- 31. Transient validation normal low flow ..... 46
- 32. Transient validation reverse low flow ..... 46
- 33. Transient validation normal high flow ..... 46

34. Transient validation reverse high flow.....	46
35. Surge case .....	49
36. Risk assessment.....	i
37. Datasheet - LD300 D-2 .....	ii
38. Datasheet - PCE-28.....	iii
39. Datasheet - CTP5000/CTR500 .....	iv
40. Datasheet - LD300 D-1 and LD300 D-0.....	v
41. Datasheet - Protran PR3202.....	vi
42. Datasheet - Orifice plate $\beta = 0.6401$ .....	vii
43. Datasheet - Orifice plate $\beta = 0.4018$ .....	viii

## List of Tables

1. Test facility orifice plate dimension and requirements .....	14
2. Test facility venturi meter dimension and requirements .....	17
3. DP transmitter test facility .....	18
4. Uncertainty section .....	24
5. Uncertainty budget - DP transmitter LD300 D-2.....	27
6. Uncertainty budget - Absolute pressure transmitter PCE-28 .....	29
7. Uncertainty budget - Temperature transmitter CTP5000/CTR5000.....	30
8. Uncertainty budget - Density .....	31
9. Uncertainty budget - Diameter Ratio.....	32
10. Uncertainty budget - Expansibility factor .....	33
11. DP transmitter evaluation.....	42
12. New DP transmitters .....	42
13. Test conditions - Transient - Low flow .....	46
14. Test conditions - Transient - High flow .....	46
15. Test condition - Surge case .....	49
16. Uncertainty budget - DP transmitter LD300 D-1.....	x
17. Uncertainty budget - DP transmitter LD300 D-0.....	xi
18. Uncertainty budget - DP transmitter Protran PR3202 .....	xii

## Nomenclature

Symbol	Description	Unit
A	Areal	m <sup>2</sup>
C	Discharge coefficient	-
D	Pipe inner diameter	m
d	Thorat/Orifice diameter	m
H	Total Head	J/kg
h	Enthalpy	
$\dot{m}$	Mass flow rate	kg/s
MW	Molecular weight	kg/kmol
$n_v$	Polytropic volume exponent	-
p	Static pressure	N/m <sup>2</sup>
Q	Volumetric flow rate	m <sup>3</sup> /s
Ra	Roughness profile	m
Re	Reynolds number	-
R <sub>o</sub>	Gas constant	8314 J/kmol K
s	Entropy	
T	Temperature	K - °C
u	Velocity	m/s
Z	Compressibility factor	-

## Greek

Symbol	Description	Unit
$\alpha$	Convergent angle	°
$\beta$	Diameter ratio	-
$\varepsilon$	Expansibility factor	-
$\Delta$	Differential	-
$\eta$	Efficiency	-
$\kappa$	Isentropic exponent	-
$\mu$	Dynamic viscosity	Pa·s
$\nu$	Specific volume	m <sup>3</sup> /kg
$\pi$	Pi	3.14159 -
$\rho$	Density	Kg/m <sup>3</sup>
$\tau$	Pressure ratio	-
$\varphi$	Divergent angle	°

## Subscript

Subscript	Description
1	Inlet
2	Discharge/Throat
3	Downstream venturi
p	Polytropic
s	Isentropic



## Abbreviations

<b>Abbreviation</b>	<b>Description</b>
ASME	The American Society of Mechanical Engineers
DP	Differential pressure
DPM	Differential pressure meter
GUM	Guide to expression of uncertainty in measurement
ISO	International Organization for Standardization
MCM	Monte Carlo Method
NTNU	Norwegian University of Science and Technology
RMS	Root mean square
RPM	Revolutions per minute
VSD	Variable Speed Drive
URL	Upper Range Limit

## Uncertainty principle

<b>Symbol</b>	<b>Description</b>
$f$	Functional relationship
$k$	Coverage factor
$n$	Number of repeated observations
$N$	Number of input quantities $X_i$
$u_c^2$	Combined variance
$u_c$	Combined standard uncertainty
$U$	Expanded uncertainty
$x$	Estimate of input quantity
$X_i$	$i$ th input quantity on which measurand $Y$ depends
$y$	Result of a measurement/output estimate
$Y$	A measurand
$\frac{\partial y}{\partial x_i}$	Sensitivity coefficient

# 1 Introduction

This chapter introduces this master’s thesis and highlights the background for the chosen topic, gives a presentation of the scope of work, and an outline of the thesis structure.

## 1.1 Background

Centrifugal compressors play a fundamental role in the current world energy situation, especially in the oil and gas industries. Due to the enormous amount of power associated with their industrial applications, even short downtime results in substantial financial losses. This places greater demands on reliable systems and the ability to prevent downtime.

A centrifugal compressor's performance is defined by its head versus inlet flow map bounded by the surge and stall regions illustrated in Figure 1. This map is critical to assess a compressor's operating range for both steady-state and transient system scenarios. Surge is a critical problem, as it can result in mechanical breakdown due to cyclical flow and pressure pulsations in the compressor. These pulsations can be violent and lead to full flow-reversal—called deep surge [1]

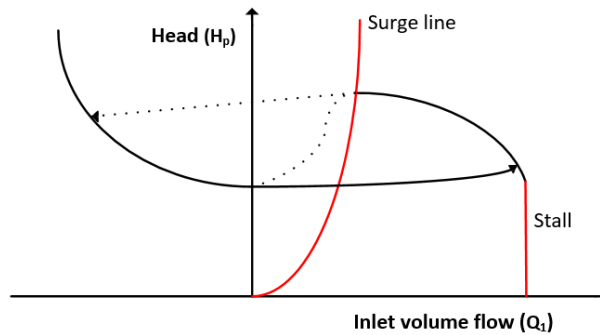


**Figure 1 The surge cycle**

Thanks to anti-surge systems surge are normally effectively prevented in the industry, controlling minimum inlet flow by recycling. However, some unpredictable transient or power supply breakdowns can generate surge before the anti-surge systems can react. Due to safe operation and the economic aspects of surge, the industry has an incentive to get better knowledge into the surge cycle phenomenon and how it should be modeled.

To correctly predict and prevent surge, dynamic process simulation models play a pivotal role. To utilize dynamic process models, reliable process data and validation of the measurement tool are necessary. This is especially relevant for the compressor inlet volume flow, which controls the compressor performance. Therefore, the focus is given to the experimental validation of the surge cycle, especially steady-state and transient inlet flow measurements.

## 1.2 Scope of work

The inlet flow at NTNU's centrifugal compressor is measured with a standard orifice plate positioned 25 m upstream of the compressor. Recently, a former student designed a portable venturi tube to fit the compressor test facility, which is placed close to the compressor inlet, allowing reverse flow measuring. To ensure that the venturi meter is measuring reverse flow and the accuracy of its measurements, the goals of the thesis are summarized below:

- Conduct an uncertainty analysis of the orifice plate.
- Validate the time delay in measurements between the orifice plate and venturi meter.
- Validate the accuracy of the venturi meter.
- Conduct a venturi meter measurement under compressor surge transients.

According to an approved standard, an uncertainty analysis of the compressor test facility orifice plate is carried out. This analysis covers mainly the steady-state flow measurements. A sensitivity analysis is presented to document how the flow uncertainties can be apportioned to different sources of uncertainty in the flow calculation input parameters. The intention is to elucidate which input parameters affect the output uncertainty the most and which changes are recommended to reduce the output's overall uncertainty.

A pressure measurement between the orifice and the venturi's differential pressure (DP) transmitter is included. The focus is to document the time delay between the two transmitters' output signals and determine if the transmitters are capable of detecting rapid pressure pulsation at the compressor inlet. By using the orifice plate as an accurate reference, the accuracy of the venturi meter in relation to the orifice plate is compared, both for normal and reverse flow. Emphasis is placed on steady-state measurements, and a venturi flow factor to correct the difference in measurements is established.

Since the venturi does not have any device to determine the flow direction, proposed solutions based on current instrumentations and flow calculations are made. Based on proposed solutions, a case within compressor surge is studied by utilizing the venturi meter.

### **1.3 Thesis structure**

Chapter 1 introduces this thesis, a description of the scope of work, and thesis structure.

Chapter 2 describes the concept of centrifugal compressor performance and presents the problem the thesis is facing.

Chapter 3 gives an overview of the flow measuring principle related to the NTNU's compressor test facility.

Chapter 4 briefly describes NTNU's compressor test facility, relevant instrumentation, and the choice behind the flow calculation.

Chapter 5 is an uncertainty and sensitivity analysis of the evaluated orifice plate, with associated results and recommendations for improvements.

Chapter 6 summarizes the work related to giving reliable flow measurements in the test facility during the investigation of the surge cycle and compressor surge case.

Chapter 7 includes a conclusion and provides recommendations for further work.

Chapter 8 presents applied references.

Chapter 9 is an Appendix including risk assessment, datasheets, sensitivity coefficients, and transmitter evaluation.

The work has been performed in NI DIAdem and Figures made in Visio.

## 2 Centrifugal compressor

The experiments presented in this thesis are based on the centrifugal compressor. The following section gives a brief description of the centrifugal compressor, the problem the industry is facing, and the focus of this thesis. Parts where no sources are specified comes from the specialization course TEP 04 "Gas Turbines and Compressors".

### 2.1 Principle

A *centrifugal compressor* is an energy-absorbing machine that adds energy to a fluid, where the purpose is to increase the pressure of the gas with centrifugal effects. The centrifugal compressor consists of a rotating impeller and a diffuser called a compressor stage. A multistage compressor consists of several stages placed one after the other. Figure 2 demonstrates a single centrifugal stage representing the NTNU's centrifugal compressor. Fluid enters the eye where it flows through the inducer in an axial direction which is the first part of the impeller. Then the radial part of the impeller accelerates the flow in the radial direction. The purpose is to transfer mechanical energy from the impeller to fluid energy (total enthalpy) in terms of increasing kinetic energy and pressure. At the exit of the impeller, the fluid enters the diffuser. The diffuser has a small increase in area, where the kinetic energy is converted to flow energy through diffusion, and one gets an increase in pressure. No work is done in the diffuser. The fluid leaves the diffuser in the radial direction and is guided to the outlet of the compressor [1].

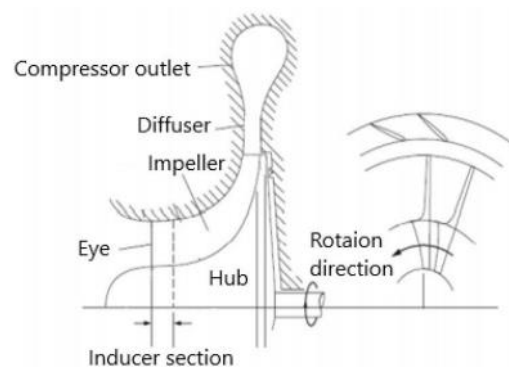


**Figure 2 Centrifugal compressor**

### 2.2 Compressor thermodynamics

To ensure that the compressors are thermodynamically assessed for the same performance, the industry utilizes the polytropic analysis. ASME PTC-10 and ISO 5389, both based on the Shultz approach [2], works as an internationally recognized standard for testing the performance of centrifugal compressors.

### 2.2.1 Performance analysis

To increase the pressure from  $P_1$  to  $P_2$ , a certain amount of energy is required. This is known as Head ( $H$ ) for a real system. It follows the real compression path from 1 to 2 and is seen in Figure 3. The isentropic head ( $H_s$ ) moves from 1 to  $2s$  and is a compression process where there is no entropy change. A polytropic analysis is used to get a better approach to the actual amount of energy required.

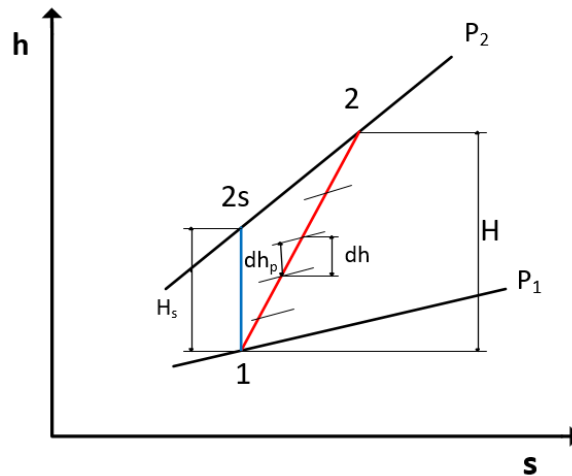


Figure 3 Compression process

The total polytropic head ( $H_p$ ) is the sum of the infinitesimal isentropic steps ( $dh_p$ ) for all the steps along the compression line:

$$H_p = \sum_1^2 dH_p \mid \text{steps} \rightarrow \infty \quad (2.1)$$

The polytropic head is then the integral of the specific volume between 1 and 2 and is defined as:

$$H_p = \int_1^2 v dp \approx \frac{n_v}{n_v - 1} [p_2 v_2 - p_1 v_1] \quad (2.2)$$

Introducing  $p v = Z R T$  and  $p v^{n_v} = \text{constant}$ , give:

$$H_p \approx \frac{n_v}{n_v - 1} \frac{Z_1 R_o T_1}{MW} \left[ \left( \frac{p_2}{p_1} \right)^{\frac{n_v}{n_v - 1}} - 1 \right] \quad (2.3)$$

The polytropic efficiency ( $\eta_p$ ) is found by the polytropic head divided by the actual head as follows:

$$\eta_p = \frac{H_p}{H} \quad (2.4)$$

### 2.3 Performance characteristic

To get a graphical representation of how the *specific* centrifugal compressor operate, a performance characteristic map is used. The shape of the performance characteristic is based on the compressors measured test condition ( $Q_1, p_1, T_1, p_2, T_2$ ) for a new compressor machine, where the polytropic head ( $H_p$ ) and polytropic efficiency ( $\eta_p$ ) plotted as a function of inlet volume flow ( $Q_1$ ). This is used as a reference when the machine is operating and as a measure of degradation and where the polytropic head characteristic forms the basis for stability and anti-surge analysis. Figure 4 shows the NTNU's compressor performance map modeled [3]. With a constant speed of 9000 RPM, the compressor efficiency will reduce when the flow rate is increased beyond, or reduced below, the best efficiency point at 1.2 m<sup>3</sup>/s.

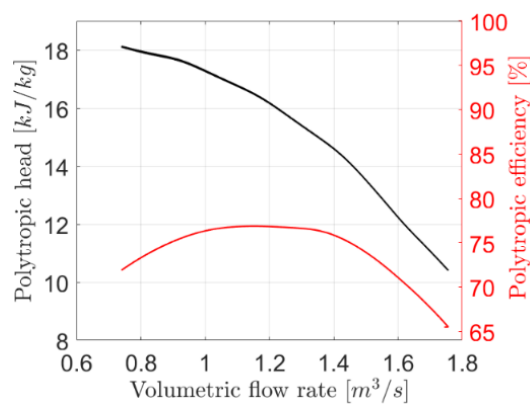


**Figure 4 Performance map NTNU's centrifugal compressor [3]**

### 2.4 Compressor system

The compressor responds according to the system, which consists of all surrounding process equipment. The compressor test facility shown in Figure 5 this includes pipes, valves, separator, pressure tank, flow meters, and safety system and forms the basis of the systems resistance curve.

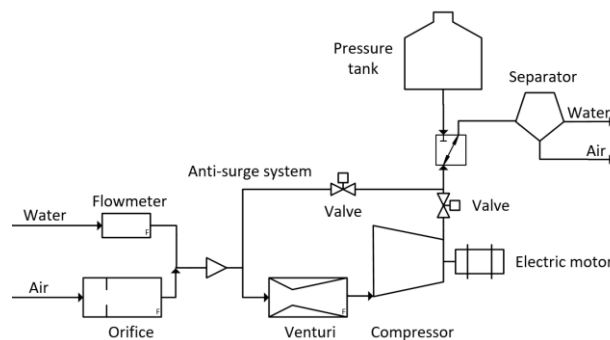


**Figure 5 PFD NTNU compressor test facility**

The interaction between the system resistance curve and performance curve pinpoints the operating point, illustrated in Figure 6. A small change in temperature, pressure, and velocities can cause the system characteristic to adjust.

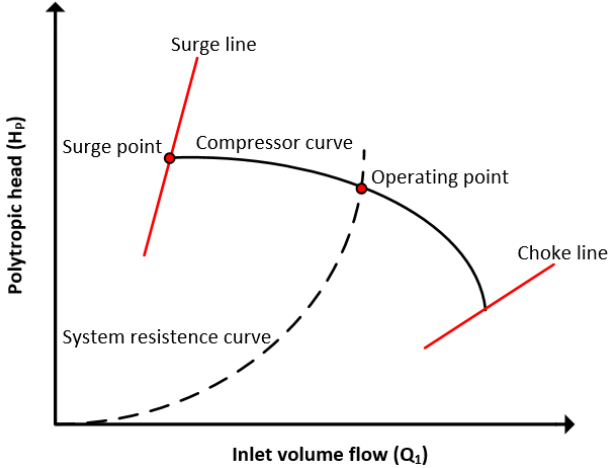


**Figure 6 Compressor system**

Understanding where the operating point is on the compressor curve is essential to avoid ending up in surge or choke. If the compressor is operated near the surge line, airfoil boundary layer separation can be created, causing turbulent flow, which can lead to airfoil stall. If a compressor is operating at a constant speed and experiences reduced flow, the downstream flow pressure can develop higher than the discharge pressure from the compressor. This will instigate the flow to re-enter the compressor ultimately and is called compressor surge.

**2.5 Surge**

With too low inlet flow rate and too high polytropic head in the performance characteristic, a major aerodynamic instability named surge can occur. The surge point at zero head rise of the characteristic curve, shown in Figure 6. When surge occurs, one can experience pressure oscillation of the flow through the compressor. Surge causes huge differences in the inlet and outlet conditions of the compressor and can generate mechanical damage to the compressor.

The surge phenomenon can be divided into different stages based on strength. The strongest and most damaging, deep surge, creates pressure oscillations large enough to reverse the flow direction periodically. The magnitude of the surge flow-reversing cycle depends on the design and operating condition of the machine but is characterized by a precipitous drop in flow [4]. The flow will typically drop from its set-point to its minimum in less than 0.05 seconds. No other physical phenomenon can cause such a drop in flow [5].



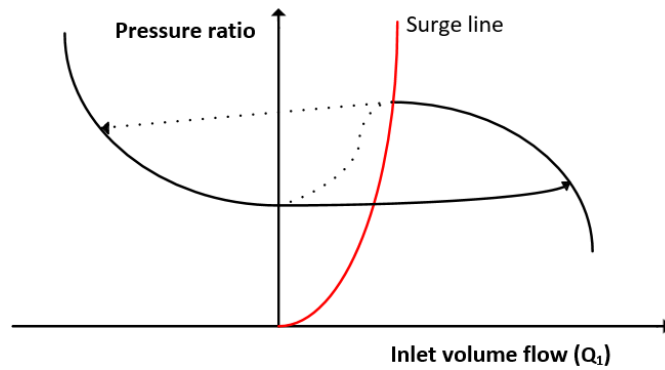


**Figure 7 The surge cycle**

The compressor performance map is suitable for steady-state and slowly changing operating conditions but is not fully applicable for rapidly transient compressor flow conditions. As surge is highly transient, involving pressure differentials across the compressor, the surge flow is a strong function not only of the compressor but also of the associated piping system. Head is then replaced with compressor pressure ratio in the performance map, illustrated in Figure 7.

Moreover, to take advantage of the compressor performance map, knowledge of the negative volume flow is essential. Substantial amounts of literature have been published to model the deep surge cycle, but all are questionable, as the accuracy of evaluated reversed volume flow is specified to be doubtful, and the test data used isn't compared to laboratory quality test data [6] [7] [8].

## **2.6 Summary and conclusion**

Surge is a highly undesirable event in the operation of a compressor, which can occur in fractions of a second. This sets high demand for the systems response time. To identify the surge cycle, both pressure ratio and flow measurement must be measured accurately. However, the compressor pressure ratio is a straightforward measurement in comparison to flow measurement. Therefore, the focus must be on the principles regarded the NTNU's compressor flow measurements in terms of accuracy, transient flow, and backflow.

### 3 Differential pressure meter

Accurate and reliable flow measurements are a critical part of determining the surge cycle and how it should be modeled. Two single-phase differential pressure meters (DPMs) are available for flow measurements, an orifice plate, and a venturi tube in the compressor test facility. This section gives an overview of the DPMs and measuring principles.

#### 3.1 Principle

DPMs obstruct the flow and thus operate by producing a difference in static pressure between the upstream and the device's throat illustrated in Figure 8.

From Bernoulli's theorem for incompressible flow in a horizontal streamline crossing the upstream and the throat planes, and conservation of mass:

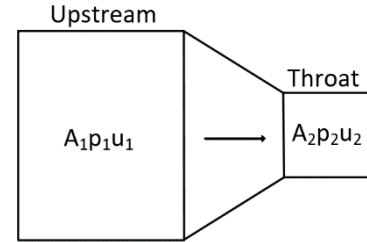


**Figure 8 Flow illustration**

$$p_1 + \frac{1}{2} \rho u_1^2 = p_2 + \frac{1}{2} \rho u_2^2 \quad (3.1)$$

$$\dot{m} = \rho A u \quad (3.2)$$

The ideal mass flow equation become:

$$\dot{m}_{ideal} = \frac{1}{\sqrt{1 - \beta^4}} \frac{\pi}{4} d^2 \sqrt{2 \Delta p \rho_1} \quad (3.3)$$

Where the diameter ratio ( $\beta$ ) is defined as  $\beta = d/D_{pipe}$ . This is an equation in which frictional pressure loss and compressibility effects are ignored. To compensate the empirical discharge coefficient  $C$  and expansibility factor  $\epsilon$  are introduced:

$$\dot{m} = \dot{m}_{ideal} \cdot C \cdot \epsilon \quad (3.4)$$

There are different methods to perform orifice flow calculation (related to  $C$  and  $\epsilon$ ), like ASME PTC 19-5 and ISO 5167. Comparisons have been made, and little difference is expected in the choice of calculation method [9]. As the venturi tube in the compressor test facility is designed in accordance with ISO 5167, this is selected.

### 3.2 Orifice plate

An *orifice plate* is a plate with a hole machined through it inserted into a pipe. As flow passes through the hole, it generates a pressure difference across the hole. The pressure tapings of the orifice plate can be installed in different positions and create the basis for flow calculation in the standard. An orifice plate manufactured according to ISO 5167 will have an uncertainty in the flow rate between 0.5 and 1 % under suitable conditions. Suitable conditions are referred to as steady-state measurements, the circularity of the bore, long enough straight lengths, customized DP transmitter, good upstream surface conditions, and edge sharpness [10].

### 3.3 Venturi tube

A *venturi tube* is a DPM consisting of an entrance cylinder, a convergent section, a throat, and a divergent section illustrated in Figure 9. For all venturi tubes, the convergent angle ( $\alpha$ ) is  $21^\circ \pm 1^\circ$ , and the divergent angle ( $\phi$ ) is in the range  $7^\circ$ – $15^\circ$ , where it is recommended that the angle is between  $7^\circ$  and  $8^\circ$ . All DPMs cause a permanent pressure loss, and the intention of the divergent section (recovery section) is to minimize the total pressure loss, where the flow follows the boundary of the tube closely. The reason the venturi tube is designed with a longer divergent section than the converging section is such that the adverse pressure gradient is too weak to invoke separation. A venturi meter is expected to have an uncertainty in the flow rate of little more than 1 % under suitable conditions [10].

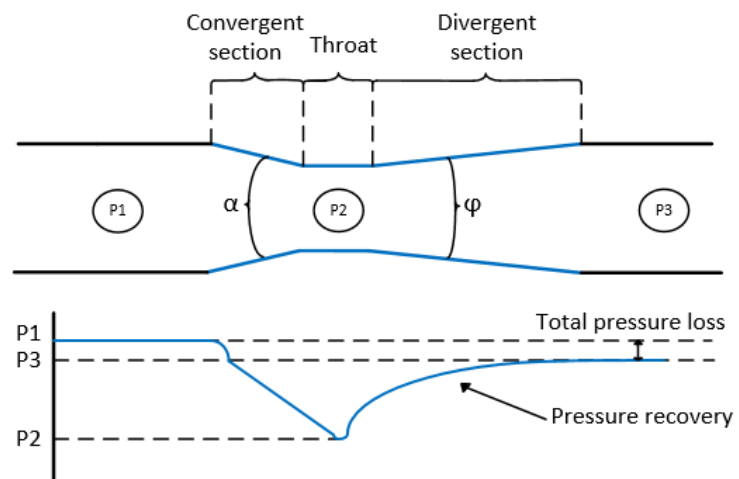


Figure 9 Venturi tube

### 3.4 Reverse flow in differential pressure meters

As the surge cycle creates negative flow, knowledge of the effect of reversing flow in the DPMs is important. Much of the published literature related to reversed flow have notable deficiencies when considered general application. In most of the literature, the DPMs are not fully described. So, no general flow-rate error correction is stated related to reversed flow in DPMs, but a significant margin of error is expected for the orifice plate [10] [11].

### 3.5 Differential pressure transmitter

Because of the square-root relationship between DP and flow rate (Equation 3.4), the DP transmitter plays a fundamental part in accuracy at low flow measurements, illustrated in Figure 10. The uncertainty of measurements increases at low flow rates with a wrongly adjusted transmitter.

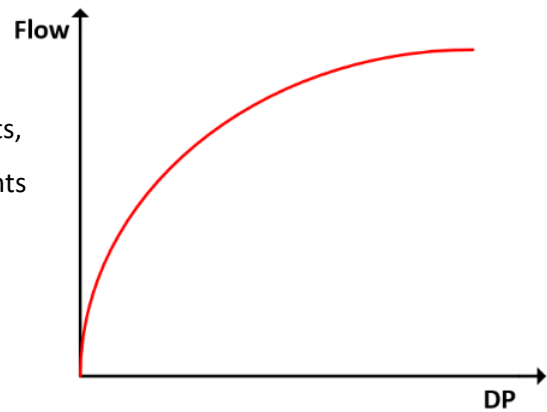


Figure 10 DP - Flow relation

The DP transmitter should also be as fast as possible during an investigating of the surge cycle. The response time is interesting when fast measurements are required and the transmitters time before the output signal reflects 99 % of the pressure change, illustrated in Figure 11. Manufacturers operate with different forms of response time, and it is important to understand the total response time of the transmitter. Most electronic DP transmitters have a time constant adjustable called damping. Damping is a delay of the output signal in relation to the measured pressure change. Damping is used where a very turbulent process pressure exists and where it is not desirable to communicate it to the control system. It is essential that damping is set to zero seconds during the surge experiment. Figure 12 illustrates how DP transmitters with different damping produce the initial precipitous drop and subsequent oscillations in flow associated with surge.

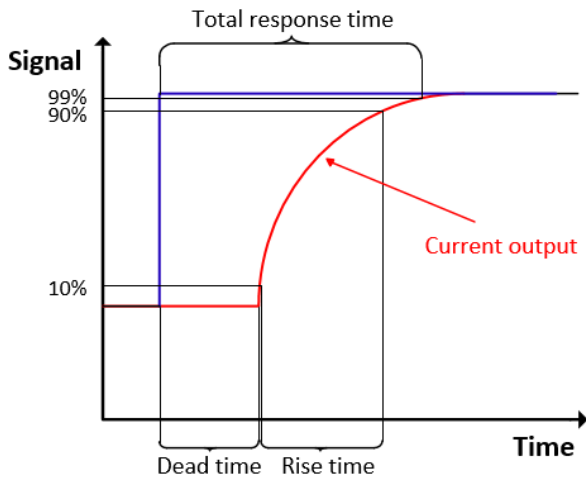


Figure 11 Response time

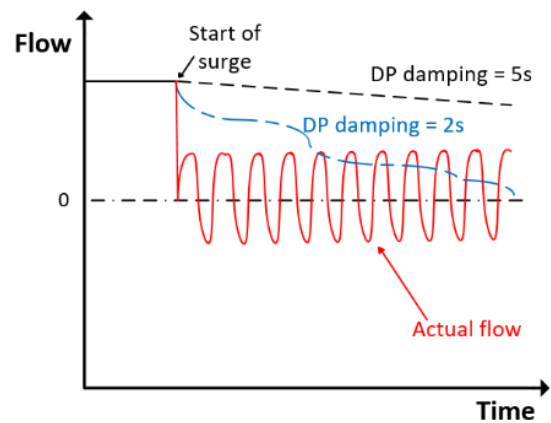
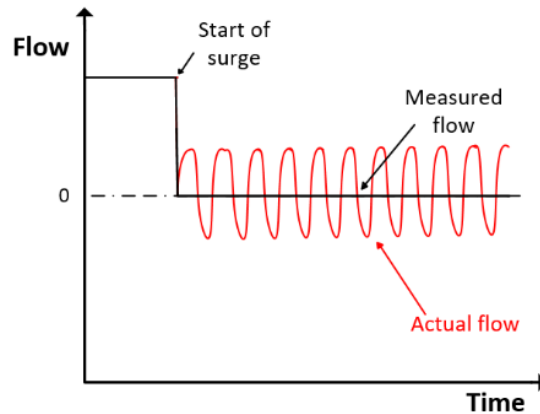


Figure 12 Damping

When a transmitter shows a particular output reading, there is a lower limit on the magnitude of the change in the measured input quantity producing an observable change in the transmitter called resolution [12]. Figure 13 shows how necessary a good resolution is when investigating low volume flow as under a surge.



**Figure 13 Resolution**

This is particularly relevant for the compressor test facility at NTNU, where low volume flow is expected (Figure 4). As low volume flow is expected, DP transmitters intended for low DP are appropriate. However, since the surge cycle can create abrupt and powerful DP values, the transmitter should have a high “max working pressure<sup>1</sup>”.

### **3.6 Summary and conclusion**

Orifice plate and venturi meter are well suited for single-phase flow metering under the right conditions. However, the measurement quality is affected by the DP transmitter, transient conditions, and reverse flow. Therefore, the focus must be directed to validate the test facility DPMs accuracy, where properly adjusted DP transmitters are installed related to surge cycle detection. Exploring how reverse flow effect the test facility DPMs under steady-state and transient conditions must also be studied before investigating the surge cycle.

---

<sup>1</sup> Max working pressure = The maximum pressure a transmitter can withstand, without being damaged.

## 4 NTNU Wet gas compressor test facility

The experiments and the thesis framework have been conducted in the wet gas compression test facility at NTNU. This section briefly describes the test facility, how the flow calculation has been performed, and which restrictions they set.

### 4.1 Compressor test facility

The test facility is located in the basement of the Department of Energy and Process Engineering at NTNU. It is an open-loop configuration consisting of a full-scale single-stage centrifugal compressor, driven by a 450 kW electric motor with a maximum rotational speed of 11000 RPM. The motor is controlled by a Variable Speed Drive (VSD). Figure 14 illustrates the test facility with the relevant components and straight lengths.

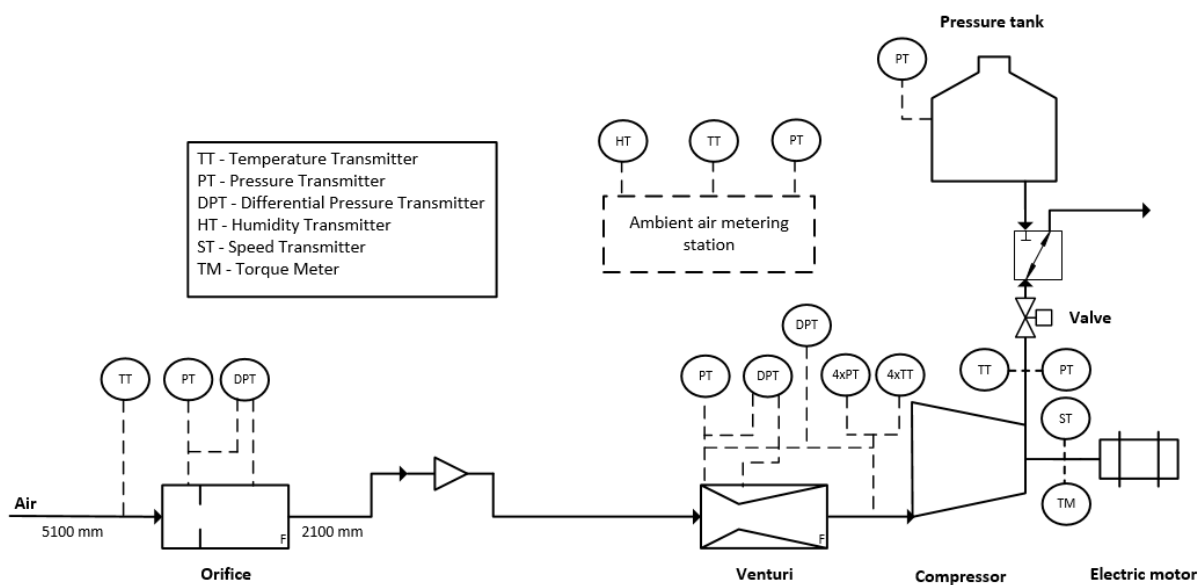


**Figure 14 PI&D of relevant equipment at compressor test facility**

The compressor utilizes low-pressure ambient air (water if necessary) as working fluid at atmospheric conditions. The volume flow of the ambient air is measured using an orifice plate delivered by AUTEK placed at the inlet pipe section. A portable venturi meter, designed by a former student, is placed close to the compressor inlet. The pipe distance between these DPMs is approximately 25 m. A 3 m<sup>3</sup> pressure tank is installed in the downstream pipe section of the compressor to provoke reverse flow if necessary. The test facility allows both steady-state and transient testing. For a deeper description of the test facility, see Bakken et. al. [13].

## 4.2 Orifice plate

The orifice plate manufactured by AUTEK has two different plates to choose between, both where the pressure tapping is installed with corner tappings.

Figure 15 illustrates the test facilities orifice plate with

mounted transmitters, and Table 1 shows the main dimensions and the requirements that should be satisfied to take advantage of ISO 5167-2 [14] flow calculation and

corresponding uncertainty. The orifice plate with installed DP transmitter are intended to measure volume flow rate at the compressor curve (Figure 4) with a DP value around 50-500 mbar depending on plate size and operating conditions.

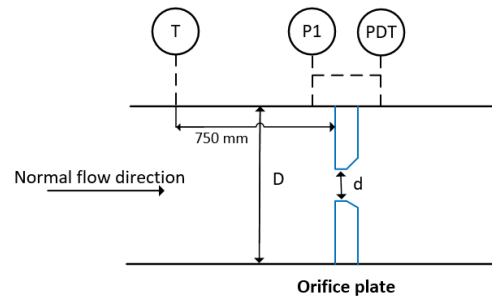


**Figure 15 Test facility orifice plate**

**Table 1 Test facility orifice plate dimension and requirements**

	Parameter	Requirements	Model	Quantity
d	Orifice diameter	$d \geq 12.5 \text{ mm}$		100.4458/160.0018 mm
D	Pipe diameter	$50 \text{ mm} \leq D \leq 1000 \text{ mm}$		250 mm
$\beta$	Diameter ratio	$0.1 \leq \beta \leq 0.75$		0.4018/0.6401
P1	Pressure		PCE-28	Range: 1.6 bar
DPT	Differential pressure		LD300 D-2	Range: 500 mbar
T	Temperature		CTP 5000	Range: -50 to 200 °C

The value of the arithmetical mean deviation of the roughness profile,  $Ra$ , shall be such that it is less than the maximum value specified in Table 1 and greater than the minimum value given in Table 2 in ISO 5167-2. As no internal roughness is measured,  $Ra$ 's approximate value is obtained from reference Table B.1 in ISO 5167-1. With a pipe material of steel welded longitudinally,  $Ra$  is  $\leq 0.03 \text{ mm}$ .

$$\frac{10^4 \cdot 0.03 \text{ mm}}{250 \text{ mm}} = 1$$

This value represents that the Reynolds number,  $Re_d$ , can be no higher than  $3 \cdot 10^5$  if the orifice beta factor ( $\beta$ ) is 0.6401 to satisfy the uncertainty values in ISO 5167-2. This value is a very conservative approach as the ISO values are not intended for precise interpolation while extrapolation is not permitted, and  $Ra$  can be smaller than 0.03 mm. With a beta factor of 0.4018, all Reynolds number is within the limit. Another point considering the surge cycle is that the flow rate has to go through zero flow before reverse. ISO 5167-2 requires the Reynolds number to be greater than 5000 to document the uncertainty.

#### 4.2.1 Flow calculation ISO 5167-2

The test facility orifice mass flow rate is determined by the following formula [14]:

$$\dot{m} = \frac{C}{\sqrt{1 - \beta^4}} \varepsilon \frac{\pi}{4} d^2 \sqrt{2\Delta p \rho_1} \quad (4.1)$$

The discharge coefficient (C) for the orifice plate equipped with corner tapings is given by the Reader-Harris/Gallagher equation:

$$C = 0.5961 + 0.0261\beta^2 - 0.216\beta^8 + 0.000521 \left( \frac{10^6 \beta}{Re_D} \right)^{0.7} \\ + (0.0188 + 0.0063A)\beta^{3.5} \left( \frac{10^6}{Re_D} \right)^{0.3} \quad (4.2)$$

Where A is given:

$$A = \left( \frac{19000\beta}{Re_D} \right)^{0.8} \quad (4.3)$$

And  $Re_D$  is the Reynolds number calculated with respect to D:

$$Re_D = \frac{4\dot{m}}{\pi \mu_1 D} \quad (4.4)$$

The expansibility factor ( $\varepsilon$ ) is determined by using the pressure ratio and the isentropic exponent for air at reference conditions,  $\kappa = 1.401$ :

$$\varepsilon = 1 - (0.351 + 0.256\beta^4 + 0.93\beta^8) \left[ 1 - \left( \frac{p_2}{p_1} \right)^{1/\kappa} \right] \quad (4.5)$$

Static DP is given between upstream and downstream pressure tapping:

$$\Delta p = p_1 - p_2 \quad (4.6)$$

The fluid density at the orifice plate is given:

$$\rho_1 = \frac{p_1}{Z_1 R T_1} \quad (4.7)$$

The volume flow is given:

$$Q_1 = \frac{\dot{m}}{\rho_1} \quad (4.8)$$



As the discharge coefficient is dependent on the Reynolds number, which itself is dependent on mass flow rate; iteration has to be done to obtain the correct mass flow rate, illustrated in Figure 16.

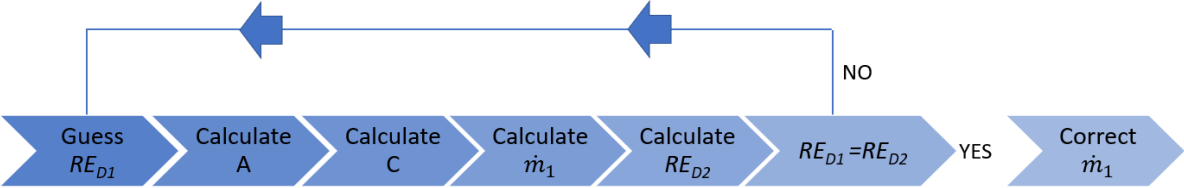


Figure 16 Orifice plate mass flow rate iteration

4.2.2 Steady-state and pulsating flow

ISO 5167 is applicable for the measurement of steady-state flow and is not suited to flows that contain any periodic flow variation or pulsation. To compensate for this, ISO 3313 [15] is used under processing pulsating flow. However, it is not valid for conditions where the flow direction becomes reverse in the measuring section. ISO 3313 defines the threshold between steady-state and pulsating flow when measuring with DP type flowmeters, where the flow can be treated as steady-state if:

$$\frac{\Delta \overline{p_p, RMS}}{\overline{\Delta p_p}} \leq 0.10 \tag{4.9}$$

Where  $\overline{\Delta p_p}$  is the time-mean value and  $\Delta \overline{p_p, RMS}$  is root mean square of the periodic DP fluctuations.

ISO 3313 states techniques for the detection and determination of pulsation flow characteristics. A technique suggested for the orifice plate is a fast-response DP transmitter. The response time of the system has to be much shorter than the time period of the pulsation in order to allow correct measurement. Otherwise, the signal will be low pass filtered. The investigation of measuring error due to pulsating flow requires a secondary instrument, and validation of pulsating flow in the test facility is not optimal due to the distance between the orifice plate and venturi meter. Thus, the focus has been directed on steady-state measurement.

### 4.3 Venturi tube

Last year a portable venturi tube was designed to fit the test facility, intended as a dry gas venturi meter according to ISO 5157-4 [16]. Figure 17 and Table 2 show the venturi with dimension and instrumentation data. In the test facility, the venturi meter operates around 0-50 mbar, depending on operating conditions. A deeper description is found in Mehlum et.al. [17].

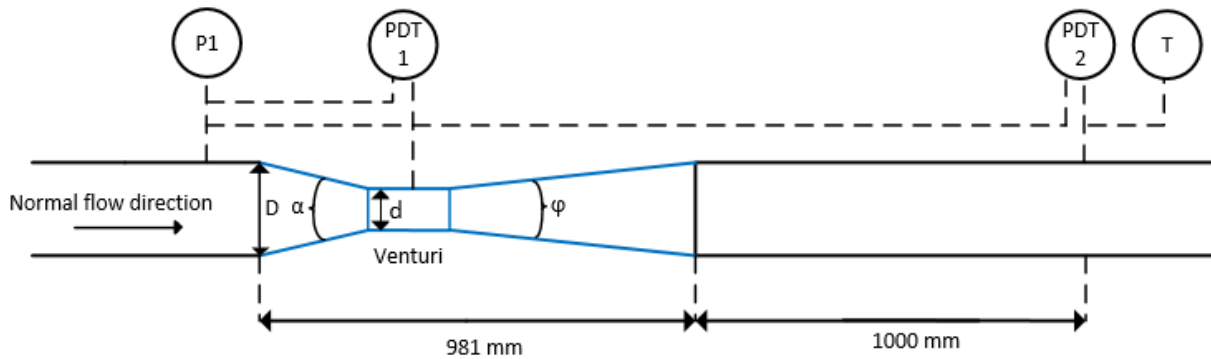


Figure 17 Test facility venturi meter

Table 2 Test facility venturi meter dimension and requirements

	Parameter	Requirements	Model	Quantity
d	Throat diameter	$20 \text{ mm} \leq d \leq 187.5 \text{ mm}$		150 mm
D	Pipe diameter	$50 \text{ mm} \leq D \leq 250 \text{ mm}$		230 mm
$\beta$	Diameter ratio	$0.4 \leq \beta \leq 0.75$		0.652
$\alpha$	Convergent angle			20.4°
$\varphi$	Divergent angle			7.4°
P1	Pressure		PCE-28	Range: 1.6 bar
DPT1	Differential pressure		LD300 D-2	Range: 500 mbar
DPT2	Differential pressure		UNIK 5000	Range: 500 mbar
T	Temperature		CTP 5000	Range: -50 to 200 °C

#### 4.3.1 Flow calculation ISO 5167-4

The test facility venturi meter mass flow rate is determined by the following formula [16]:

$$\dot{m} = \frac{C}{\sqrt{1 - \beta^4}} \varepsilon \frac{\pi}{4} d^2 \sqrt{2 \Delta p \rho_1} \quad (4.10)$$

The discharge coefficient (C) is given for different size of venturi meter and type of convergent section. The venturi at NTNU has a C = 0.995, with a relative uncertainty of ±1 %. The expansibility factor ( $\epsilon$ ) is determined by using the isentropic exponent for air,  $\kappa = 1.401$  and the pressure ratio  $\tau$  ( $p_2/p_1$ ):

$$\epsilon = \sqrt{\left(\frac{\kappa\tau^{2/\kappa}}{\kappa - 1}\right)\left(\frac{1 - \beta^4}{1 - \beta^4\tau^{2/\kappa}}\right)\left(\frac{1 - \tau^{(\kappa-1)/\kappa}}{1 - \tau}\right)} \quad (4.11)$$

The static pressure difference exists between the upstream section and the throat section of the venturi:

$$\Delta p = p_1 - p_2 \quad (4.12)$$

Density is measured at venturi inlet:

$$\rho_1 = \frac{p_1}{Z_1RT_1} \quad (4.13)$$

The volume flow is given:

$$Q = \frac{\dot{m}}{\rho_1} \quad (4.14)$$

#### 4.4 Instrumentation data

The instrumentation of the test facility is performed in accordance with ASME PTC-10, where the data acquisition system is based on National Instrument PXI ensures time consistent measurements up to 20 kHz. To ensure the validity of the relevant instrumentation, calibration has been performed by the author<sup>2</sup>. Both the orifice plate and venturi meter use the LD300 D-2 as DP transmitter, but where the orifice DP transmitter is ten years old compared to the one-year-old venturi transmitter. The DP transmitters are “smart cells”, where it is possible to change the span<sup>3</sup>. Table 3 shows the main DP instrumentation data.

**Table 3 DP transmitter test facility**

Parameter	Quantity
Total response time	100 ms
Damping	0 ms
Resolution	0.023 mbar

<sup>2</sup> The calibration is not valid in an uncertainty analysis as the calibration instrument has no documented certificate and is intended as a check of the instrumentation.

<sup>3</sup> Span = The transmitters' work range, set by the user. Must be equal to the range or smaller.

#### **4.5 Risk assessment**

Risk assessment was performed before conducting the experiments following the department's procedure. A form for Risk assessment is given in Appendix A. Co-supervisor Erik Langørgen was responsible for driving the compressor and verifying that operating parameters appeared within limits.

#### **4.6 Summary and conclusion**

The venturi meter is most suited to measure the surge cycle in the test facility due to its location. However, an appropriate measurement validation against the manufacture orifice plate with documented accuracy is necessary to determine its performance. As the orifice plate and venturi meter have 25 m with pipe (of different material) between them, the main objective is steady-state validation. As reverse flow is expected in the surge cycle, resulting in low flow, there are limitations in the flow calculations related to document the uncertainty.

## 5 Uncertainty and sensitivity analysis

Establishing accurate and reliable flow measurements is paramount, as they form a necessary basis for investigating the surge cycle. The objective is to utilize the venturi meter located directly upstream of the compressor, where it also has reliable flow measurement at reverse flow. To validate the venturi meter a reliable reference is needed. The standard orifice plate manufacture by AUTEK is regarded as a reliable reference if the uncertainty is documented.

This chapter will then present an uncertainty analysis of the orifice plate at the compressor test facility. Furthermore, a sensitivity analysis has been performed to evaluate how uncertainties in the output can be appointed to different sources of uncertainty in the inputs, thus identifying the main contributors to the uncertainties. Finally, suggestions for improvements of the uncertainty related to surge experiments will be made based on available offers and opportunities.

## 5.1 Uncertainty analysis

All measurements include errors. The error in a measurement is specified as the difference between the measured value and the actual value of the physical property in question. This error is usually not known but can be approximated by utilizing an uncertainty analysis. The analysis is a numeric methodical approach, defining the potential error that is present in all data. From the uncertainty analysis, it is possible to obtain a confidence interval where the actual value will be placed within a specified probability. All errors must be determined at the same confidence interval, where the industry uses 95 % as the standard probability of the confidence interval [18] [19] [20].

There are different standards to present the uncertainty, like AMSE PTC 19.1 and ISO 98. The most recognized international standard for evaluating uncertainty is the Guide to expression of uncertainty in measurement (GUM), presented in ISO 98. The GUM gives three different methods to identify the uncertainty:

- Type A
- Type B
- The Monte Carlo Method (MCM)

Probability distributions are the basis of both Type A and Type B evaluation in GUM, where standard deviations and variance specify the uncertainty components. Type A evaluation estimate the variance with a statistical method of the data obtained by direct measurements, while Type B is calculated by decision using all related information on the variability of the uncertainty, such as:

- Manufactures specification.
- Calibration certificates.
- Previous measurement data.
- Uncertainties assigned to reference data taken from handbooks.

The MCM is an alternative numerical method to Type A and Type B evaluation, where the standard uncertainty might be unreliable and unrealistic coverage intervals might be the outcome [20] [21] [22].

A prerequisite for doing a valid Type A evaluation is identical measurement conditions, which are not guaranteed in the test facility. This thesis focuses on the Type B evaluation as the information related to standard uncertainty is available.

### 5.1.1 Type B evaluation

The general implementation of Type B evaluation is defined as:

The measurand  $Y$  (output quantity) is mostly not measured directly, but determined from  $N$  other quantities,  $X_1, X_2, \dots, X_N$  through a functional relationship  $f$ :

$$Y = f(X_1, X_2, \dots, X_N) \quad (5.1)$$

$y$  symbolizes the estimate of the measurand  $Y$  and the input estimates  $x_1, x_2, \dots, x_n$  symbolizes the input quantities  $X_1, X_2, \dots, X_N$ . Thus, the output estimate  $y$ , which is the result of the measurement, is defined as:

$$y = f(x_1, x_2, \dots, x_n) \quad (5.2)$$

If the input estimate  $x_i$  is taken from a manufactures specification and the quoted uncertainty is stated to be a particular multiple of a standard deviation, the standard uncertainty  $u(x_i)$  is the quoted value divided by the multiplier. If the quoted uncertainty of  $x_i$  is not given in as a multiple of standard deviation, one may assume a normal distribution.

The combined standard uncertainty  $u_c(y)$ , is the positive square root of the combined variance  $u_c^2(y)$ . This is based on that all input quantities are independent and not correlated with each other.

$$u_c^2(y) = \sum_{n=1}^n \left( \frac{\partial f}{\partial X_i} \right)^2 u^2(X_i) \quad (5.3)$$

$$u_c(y) = \sqrt{\sum_{n=1}^n \left( \frac{\partial f}{\partial X_i} \right)^2 u^2(X_i)} \quad (5.4)$$

The partial derivatives  $\frac{\partial y}{\partial x_i}$  are often called sensitivity coefficients and describes how the output estimate  $y$  varies with changes in the value of the input estimates  $x_1, x_2, \dots, x_i$ . To define the expanded uncertainty denoted by  $U$ , which is an interval around the measurement result based on the required confidence level, the standard uncertainty of the output estimate,  $u(y)$  is multiplied with a convergence factor.

$$U = k \cdot u_c(y) \quad (5.5)$$

A flow chart presented in Figure 18 represents the Type B evaluation.

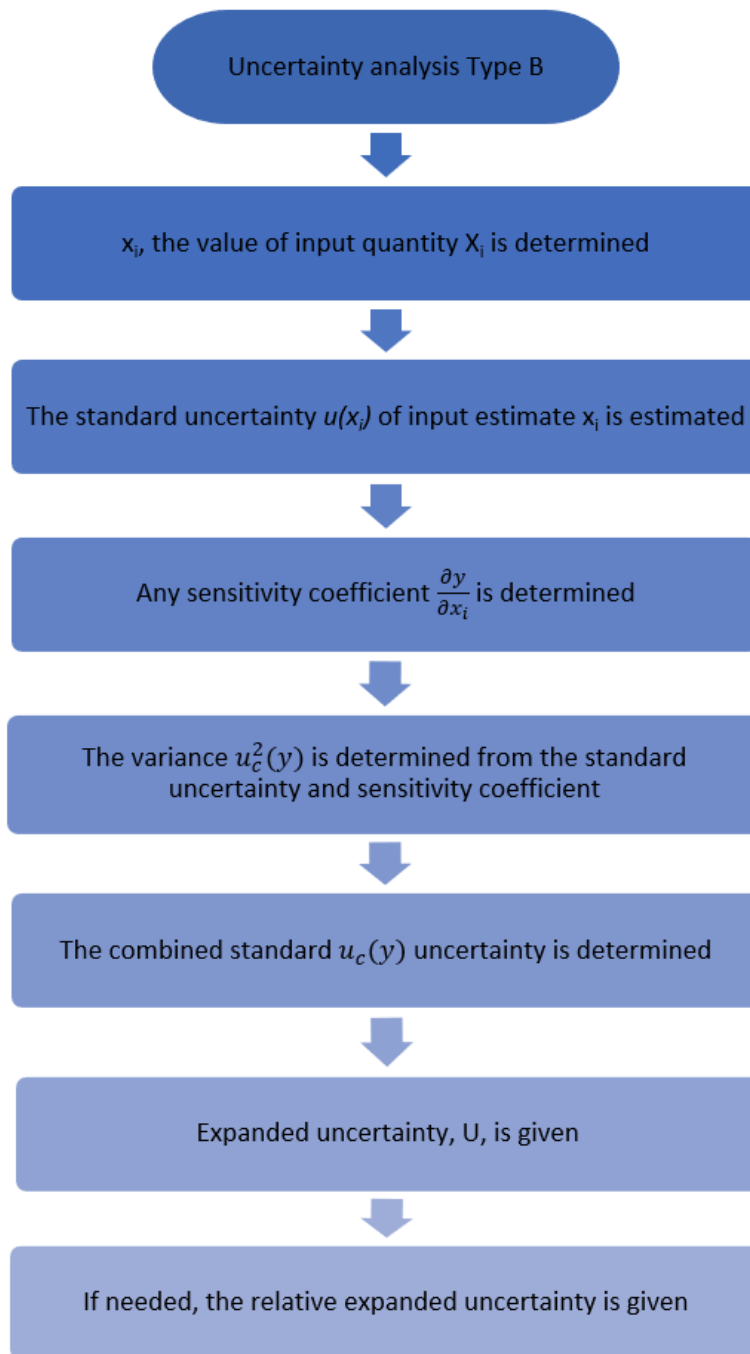


**Figure 18 Type B evaluation**



## 5.2 Orifice uncertainty analysis

An uncertainty analysis is carried out on the orifice plate with beta factor ( $\beta$ ) equal 0.6401. A description of each component in the orifice plate calculation is presented. Not all uncertainty budgets will be filled in as some parameter depends on operating conditions. ISO 5167-1 [23] give the specific working formula for relative expanded uncertainty of the mass flow rate:

$$\frac{U\dot{m}}{\dot{m}} = \sqrt{\left(\frac{UC}{C}\right)^2 + \left(\frac{U\varepsilon}{\varepsilon}\right)^2 + \left(\frac{2\beta^4}{1-\beta^4}\right)^2 \left(\frac{UD}{D}\right)^2 + \left(\frac{2}{1-\beta^4}\right)^2 \left(\frac{Ud}{d}\right)^2 + \frac{1}{4}\left(\frac{U\Delta p}{\Delta p}\right)^2 + \frac{1}{4}\left(\frac{U\rho_1}{\rho_1}\right)^2} \quad (5.6)$$

The uncertainty to discharge coefficient ( $C$ ) and expansibility factor ( $\varepsilon$ ) is given in ISO 5167-2 [14], while the other parameters ( $\beta$ ,  $D$ ,  $d$ ,  $\Delta p$  and  $\rho_1$ ) are determined by the test facilities orifice plate specification. As some parameters depend on others, they are presented in the order listed in Table 4.

**Table 4 Uncertainty section**

Parameter	Covered in section
Differential pressure ( $\Delta p$ )	5.2.1
Density ratio ( $\rho_1$ )	5.2.2
Pipe diameter ( $D$ )	5.2.3
Orifice diameter ( $d$ )	5.2.3
Diameter ratio ( $\beta$ )	5.2.3
Expansibility factor ( $\varepsilon$ )	5.2.4
Discharge coefficient ( $C$ )	5.2.5

### 5.2.1 Differential pressure transmitter

The DP transmitter installed at the orifice plate is an LD300 D-2 from Smar technology company, with an Upper Range Limit<sup>4</sup> (URL) on 500 mbar and an adjustable span. Essential parameters from the datasheet are extracted and presented. The datasheet is listed in Appendix B.1.

#### 1. Pressure transmitter uncertainty, $u(\Delta\hat{P}_{Transmitter})$ :

The manufacturer's uncertainty specification (0.075 % of span) is used as a conservative approach, where the linearity, hysteresis, and repeatability effects are included. If the DP transmitter had been calibrated with documented uncertainty, the transmitter uncertainty could be further reduced. The span is set from -50 to 200 mbar, i.e. 250 mbar, gives a standard uncertainty:

$$u(\Delta\hat{P}_{Transmitter}) = \frac{0.00075 \cdot 250}{2} = 0.094 \text{ mbar}$$

#### 2. Stability, $u(\Delta\hat{P}_{Stability})$ :

The manufacturer's stability represents an increasing or decreasing offset in the readings with time and is given as 0.1 % of URL for 24 months. Based on the DP transmitter is valid every two years, the standard uncertainty of the transmitter caused by stability becomes:

$$u(\Delta\hat{P}_{Stability}) = \frac{[(0.001 \cdot 500) \cdot \frac{2}{2}]}{2} = 0.250 \text{ mbar}$$

#### 3. Temperature effect, $u(\Delta\hat{P}_{Temperature\ effect})$ :

The manufacturer specifies a temperature effect as (0.02 % URL + 0.1 % span) per 20 °C temperature change. Temperature change is referred to as a change in ambient temperature relative to the ambient calibration temperature. Since the transmitter is not calibrated with a valid calibration process, the ambient calibration temperature is set to 25 °C as specified in the datasheet.

---

<sup>4</sup> URL = Transmitter upper measurement range, given by the manufacturer.

Ambient temperature will gradually increase during testing. In the “worst-case” scenario, the transmitter is exposed to a temperature of 30 °C. With a calibration temperature equal to 25 °C, the max temperature change is 5 °C. The standard uncertainty due to temperature effect then becomes:

$$u(\Delta\hat{P}_{Temperature\ effect}) = \frac{[(0.0002 \cdot 500 + 0.001 \cdot 250) \cdot \frac{5}{20}]}{2} = 0.044\ mbar$$

#### 4. Static pressure effects, $u(\Delta\hat{P}_{Static\ pressure\ effects})$ :

The static pressure effect consists of two types of errors, zero and span. Zero error is a systematic error that can be eliminated with a valid calibration. In this analysis, the uncertainty is considered as the most conservative approach, where the manufacturer datasheet specifies the uncertainty to  $\pm 0.1\%$  URL per 7 MPa. This means that the operating conditions affect the standard uncertainty:

$$u(\Delta\hat{P}_{Zero\ error}) = \frac{[(0.001 \cdot 500) \cdot \frac{Operating\ pressure}{7 \cdot 10^4}]}{2} = y\ mbar$$

Span error is in the manufacturer sheet given as  $\pm 0.2\%$  of reading per 7 MPa, and the size of the standard uncertainty become:

$$u(\Delta\hat{P}_{Span\ error}) = \frac{(0.002 \cdot \frac{Operating\ pressure}{7 \cdot 10^4})}{2} = y\ mbar$$

#### 5. Power supply and mounting position effects:

The manufacturer datasheet specifies the power supply effect as  $\pm 0.005\%$  of calibrated span per volt. Due to this uncertainty representing a small value, this value is insignificant.

Mounting position effects are due to the transmitter consisting of oil-filled fluid and may influence the uncertainty if the transmitter is incorrectly attached. This thesis assumes that the transmitter was installed correctly.

**Table 5 Uncertainty budget - DP transmitter LD300 D-2**

Source	Input uncertainty				Combined uncertainty	
	Expanded uncertainty	Confidence level	Con. factor $k$	Standard uncertainty	Sens. coeff.	Variance
Transmitter uncertainty	0.188 mbar	95 %	2	0.094 mbar	1	0.008 (mbar) <sup>2</sup>
Stability	0.500 mbar	95 %	2	0.250 mbar	1	0.063 (mbar) <sup>2</sup>
Temperature effect	0.088 mbar	95 %	2	0.044 mbar	1	0.002 (mbar) <sup>2</sup>
Static pressure effects	*	95 %	2	*	1	*
Sum of variance					$u_c^2(\Delta\hat{P})$	0.073 mbar+*
Combined standard uncertainty					$u_c(\Delta\hat{P})$	0.271 mbar+ $\sqrt{*}$
Expanded uncertainty (95 % confidence level, $k = 2$ )					$U(\Delta\hat{P})$	0.541 mbar+ $2\sqrt{*}$
Operating DP					$\Delta\hat{P}$	X
Relative expanded uncertainty (95 % confidence level)					$U(\Delta\hat{P})/\Delta\hat{P}$	(0.541 mbar+ $2\sqrt{*}$ )/X

\* Will change according to the operating conditions.

### 5.2.2 Density

The density at the orifice plate inlet is given:

$$\rho_1 = \frac{p_1}{Z_1 RT_1} \quad (5.7)$$

The pressure is measured with an absolute pressure transmitter PCE-28, and the temperature is measured with a CTP5000 thermometer probe connected to a CTR5000 precision thermometer. The most significant inaccuracy should always be used where several devices produce the output signal. With pressure lower than 10 bar and normal operating temperature, the conditions are considered ideal, and Z is set to 1.

#### **Absolute pressure transmitter PCE-28:**

The most important parameters from the datasheet are extracted and presented, where the datasheet is listed in Appendix B.2.

##### **1. Pressure transmitter uncertainty, $u(\hat{P}_{Transmitter})$ :**

The manufactures uncertainty specification (0.2 % of range) is used as a conservative approach, if the transmitter had been calibrated, the transmitter uncertainty could be further reduced. The transmitter range is from 0 to 1.6 bar and gives a standard uncertainty:

$$u(\hat{P}_{Transmitter}) = \frac{0.002 \cdot 1.6}{2} = 0.002 \text{ bar}$$

##### **2. Stability, $u(\hat{P}_{Stability})$ :**

The transmitter stability (0.1 % of range/year) is affected by the years between calibration. The transmitter was installed ten years ago and has not been calibrated since. The standard uncertainty caused by stability becomes:

$$u(\hat{P}_{Stability}) = \frac{[(0.001 \cdot 1.6) \cdot \frac{10}{1}]}{2} = 0.008 \text{ bar}$$

##### **3. Temperature effect, $u(\hat{P}_{Tempertaure \text{ effect}})$ :**

The manufactures specify a temperature effect as ( $\pm 0.2$  % range) per 10 °C temperature change. Temperature change is referred to as the change in ambient temperature relative to the ambient calibration temperature. Since the transmitter is not calibrated, the ambient calibration temperature is set to 25 °C as specified in the datasheet.

Ambient temperature will gradually increase during testing. In the “worst case” scenario the transmitter is exposed to a max temperature of 30 °C. With a calibration temperature equal to 25 °C, the max temperature change is 5 °C. The standard uncertainty due to temperature effect then becomes:

$$u(\hat{P}_{Temperature\ effect}) = \frac{[(0.002 \cdot 1.6) \cdot \frac{5}{10}]}{2} = 8.00 \cdot 10^{-4}\ bar$$

**4. Hysteresis and repeatability,  $u(\hat{P}_{Hysteresis\ and\ repeatability})$ :**

Hysteresis and repeatability are not included in the transmitter accuracy and is specified as 0.05 % of range in the datasheet. The standard uncertainty due to hysteresis and repeatability is thus:

$$u(\hat{P}_{Hysteresis\ and\ repeatability}) = \frac{(0.0005 \cdot 1.6)}{2} = 4.00 \cdot 10^{-4}\ bar$$

**Table 6 Uncertainty budget - Absolute pressure transmitter PCE-28**

Source	Input uncertainty				Combined uncertainty	
	Expanded uncertainty	Confidence level	Con. factor $k$	Standard uncertainty	Sens. coeff.	Variance
Transmitter uncertainty	0.003 bar	95 %	2	0.002 bar	1	$2.56 \cdot 10^{-6}\ (bar)^2$
Stability	0.016 bar	95 %	2	0.008 bar	1	$6.40 \cdot 10^{-5}\ (bar)^2$
Temperature effect	0.002 bar	95 %	2	$8.00 \cdot 10^{-4}$ bar	1	$6.40 \cdot 10^{-7}\ (bar)^2$
Hysteresis and repeatability	$8.00 \cdot 10^{-4}$ bar	95 %	2	$4.00 \cdot 10^{-4}$ bar	1	$1.60 \cdot 10^{-7}\ (bar)^2$
Sum of variance						$6.66 \cdot 10^{-5}\ (bar)^2$
Combined standard uncertainty						0.008 bar
Expanded uncertainty (95 % confidence level, $k = 2$ )						0.016 bar
Operating pressure						X
Relative expanded uncertainty (95 % confidence level)						$(0.016\ bar/X)$

## Thermometer CTP5000/CTR5000

The most important parameters from the datasheet are extracted and presented, where the datasheet is listed in Appendix B.3.

### 1. Temperature transmitter uncertainty, $u(\hat{T}_{Thermometer})$ :

The temperature manufactures uncertainty specification (0.01 K) is used as a conservative approach, since the thermometer is not calibrated, gives a standard uncertainty:

$$u(\hat{T}_{Thermometer}) = \frac{0.01}{2} = 0.005 \text{ K}$$

### 2. Stability, $u(\hat{T}_{Stability})$ :

The temperature probe stability (10 mK per year) is determined on the years between each calibration. Since the temperature probe is not calibrated after installation, three years is set, and the standard uncertainty caused by stability becomes:

$$u(\hat{T}_{Stability}) = \frac{(0.01) \cdot \frac{3}{1}}{2} = 0.015 \text{ K}$$

**Table 7 Uncertainty budget - Temperature transmitter CTP5000/CTR5000**

Source	Input uncertainty				Combined uncertainty	
	Expanded uncertainty	Confidence level	Con. factor $k$	Standard uncertainty	Sens. coeff.	Variance
Transmitter uncertainty	0.010 K	95 %	2	0.005 K	1	$2.50 \cdot 10^{-5} \text{ (K)}^2$
Stability	0.030 K	95 %	2	0.015 K	1	$2.25 \cdot 10^{-4} \text{ (K)}^2$
Sum of variance						$2.50 \cdot 10^{-4} \text{ (K)}^2$
Combined standard uncertainty						0.016 K
Expanded uncertainty (95 % confidence level, $k = 2$ )						0.032 K
Operating temperature						X
Relative expanded uncertainty (95 % confidence level)						$(0.032 \text{ K}/X)$

**Table 8 Uncertainty budget - Density**

Source	Input uncertainty				Combined uncertainty	
	Expanded uncertainty	Confidence level	Con. factor $k$	Standard uncertainty	Sens. coeff.	Variance
Pressure transmitter	1600 Pa	95 %	2	800 Pa	Eq. 1 <sup>^</sup>	*
Temperature transmitter	0.032 K	95 %	2	0.016 K	Eq. 2 <sup>^</sup>	*
Sum of variance					$u_c^2(\hat{\rho})$	*
Combined standard uncertainty					$u_c(\hat{\rho})$	*
Expanded uncertainty (95 % confidence level, $k = 2$ )					$U(\hat{\rho})$	*
Operating density					$\hat{\rho}$	*
Relative expanded uncertainty (95 % confidence level)					$U(\hat{\rho})/\hat{\rho}$	*

\* Will change according to the operating conditions.

<sup>^</sup> The sensitivity coefficient is listed in Appendix C.



### 5.2.3 Diameter ratio

From the orifice plate datasheet given in Appendix B.6 the relative expanded uncertainty to pipe diameter (D) and orifice diameter (d) is specified as:

$$\left(\frac{UD}{D}\right) = 0.30 \% = 0.75 \text{ mm} \quad (5.8)$$

$$\left(\frac{Ud}{d}\right) = 0.05 \% = 0.08 \text{ mm} \quad (5.9)$$

**Tabel 9 Uncertainty budget - Diameter Ratio**

Source	Input uncertainty				Combined uncertainty	
	Expanded uncertainty	Confidence level	Con. factor $k$	Standard uncertainty	Sens. coeff.	Variance
Pipe diameter	$7.50 \cdot 10^{-4} \text{ m}$	95 %	2	$3.75 \cdot 10^{-4} \text{ m}$	1	$1.41 \cdot 10^{-7} (\text{m})^2$
Orifice diameter	$8.00 \cdot 10^{-5} \text{ m}$	95 %	2	$4.00 \cdot 10^{-5} \text{ m}$	1	$1.60 \cdot 10^{-9} (\text{m})^2$
Sum of variance						$1.43 \cdot 10^{-7} (\text{m})^2$
Combined standard uncertainty						$3.78 \cdot 10^{-4} \text{ m}$
Expanded uncertainty (95 % confidence level, $k = 2$ )						$7.55 \cdot 10^{-4} \text{ m}$
Operating diameter ratio						0.6401
Relative expanded uncertainty (95 % confidence level)						0.118 %

## 5.2.4 Expansibility factor

$$\varepsilon = 1 - (0.351 + 0.256\beta^4 + 0.93\beta^8) \left[ 1 - \left( \frac{p_1 - \Delta p}{p_1} \right)^{1/\kappa} \right] \quad (5.10)$$

ISO 5167-2 [14] stated that when  $\beta$ ,  $p_1$ ,  $\Delta p$  and  $k$  are assumed to be known without error, the relative expanded uncertainty of the expansibility factor is equal to:

$$\left( \frac{U\varepsilon}{\varepsilon} \right) = 3.5 \frac{\Delta p}{\kappa p_1} \% \quad (5.11)$$

Both  $\beta$ ,  $p_1$ ,  $\Delta p$  and  $k$  have a small error so an uncertainty budget shall in principle be used. The sensitivity coefficients are listed in Appendix C.

**Tabel 10 Uncertainty budget - Expansibility factor**

Source	Input uncertainty				Combined uncertainty	
	Expanded uncertainty	Confidence level	Con. factor $k$	Standard uncertainty	Sens. coeff.	Variance
Diameter ratio	$7.55 \cdot 10^{-4}$ m	95 %	2	$3.76 \cdot 10^{-4}$ m	Eq. 3	*
Static pressure transmitter	0.016 bar	95 %	2	0.008 bar	Eq. 4	*
DP transmitter	*	95 %	2	*	Eq. 5	*
Isentropic exponent	-**	95 %	2	-	-	-
ISO	Eq. 5.11*	95 %	2	*	1	*
Sum of variance	$u_c^2(\hat{\varepsilon})$					*
Combined standard uncertainty	$u_c(\hat{\varepsilon})$					*
Expanded uncertainty (95 % confidence level, $k = 2$ )	$U(\hat{\varepsilon})$					*
Operating expansibility factor	$\hat{\varepsilon}$					*
Relative expanded uncertainty (95 % confidence level)	$U(\hat{\varepsilon})/\hat{\varepsilon}$					*

\* Will change according to the operating conditions.

\*\*With small temperature and pressure changes at the orifice plate the isentropic exponent is set to 1.401 with zero expanded uncertainty.

### 5.2.5 Discharge coefficient

ISO 5167-2 [14] stated that when  $\beta$ ,  $D$ ,  $Re_D$  and  $Ra/D$  are assumed to be known without error, the relative uncertainty of the discharge coefficient is equal to:

$$\left(\frac{UC}{C}\right) = 0.5 \% (\beta = 0.4018) \quad (5.12)$$

$$\left(\frac{UC}{C}\right) = 1.66\beta - 0.5 \% (\beta = 0.6401) \quad (5.13)$$

Since  $\beta$ ,  $D$ ,  $Re_D$  and  $Ra/D$  have a small error, so an uncertainty budget shall in principle be used. As equation 5.12/5.13 is referred to as the dominant factor [24] the remaining error can be eliminated. When  $Re$  is smaller than 10000, a relative uncertainty of 0.5 % is added to equation 5.12/5.13.

#### Installation requirements

As ISO 5167-2 sets installation requirements for the orifice plate to get a swirl-free flow, an assessment of the test facility orifice plate installation is necessary. The installation requirements will affect the discharge coefficient. There are three main parts to consider, upstream and downstream straight length and circularity of the pipe. Whether the installation contains a flow conditioner upstream or downstream of the orifice plate is decisive for which table to use. Since the orifice plate includes neither a flow conditioner upstream nor downstream, Table 3 in ISO 5167-2 should be followed.

Since the air intake is 5100 mm upstream of the orifice plate and represents an abrupt symmetrical reduction, an additional uncertainty of 0.5 % should be added arithmetically to the uncertainty in the discharge coefficient described in Table 3 in ISO 5167-2. The thermometer placed 750 mm upstream of the orifice plate will also affect the flow, as it creates a flow pocket behind the thermometer. With a thermometer probe diameter of 6 mm and a distance of 75 mm upstream of the orifice plate, 0.5 % additional uncertainty shall be added. It specifies that the thermometer pocket will not alter the required minimum straight upstream lengths, and the total added uncertainty related to upstream fittings is 0.5 %.

With closest fittings 2100 mm downstream of the orifice plate, no additional uncertainty should be added. The circular limit is set to 2·D measured from the orifice plate's upstream face and should differ no more than 3 % from the orifice plate's mean diameter downstream. As the pipe has a slight change in diameter 2700 mm from the face, there is no additional uncertainty.

### 5.3 Orifice uncertainty analysis result

Figure 19 shows the result of the current test facility orifice plate installation relative expanded uncertainty (convergence factor = 2) as a function of mass flow rate. It can be seen that the orifice plate has a rapid increase in relative expanded uncertainty as the mass flow rate decreases below 0.5 kg/s, while a mass flow rate higher than 1.5 kg/s gives a constant relative expanded uncertainty of 1.23 %. Further, the DP transmitter resolution sets the minimum achievable mass flow measurement value to 0.06 kg/s.

The compressor speed and discharge throttle valve were utilized to regulate the orifice plate mass flow rate. Since the mass flow rate is used to validate the venturi meter, it will be the basis for the uncertainty analysis and not the obvious volume flow rate (related to compressor performance and surge cycle)

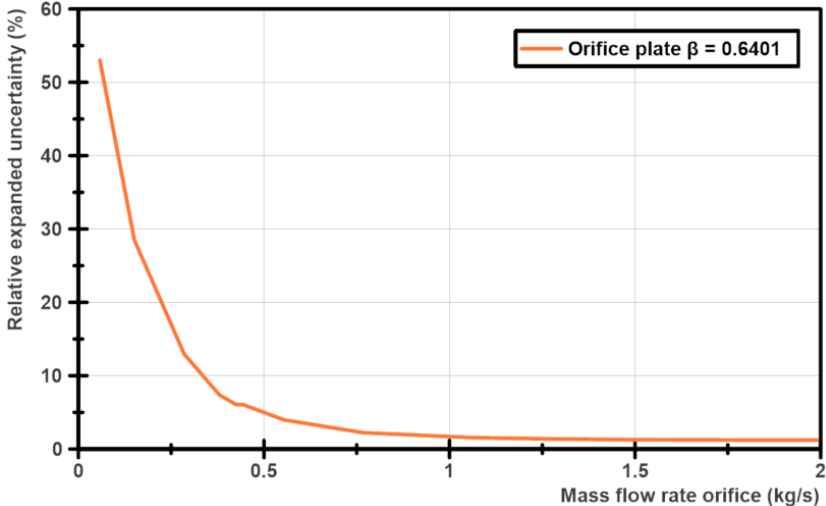


Figure 19 Orifice plate relative expanded uncertainty

#### Summary and conclusion

Establishing accurate and reliable flow measurement is paramount, as it forms a necessary basis for investigating the surge cycle phenomenon and model simulation. An experimental uncertainty analysis of the orifice plate at the test facility was conducted to analyze the uncertainty at different flow rates.

The analysis shows that the existing test facility orifice plate provides a considerable relative expanded uncertainty at low flow rates. This was also expected as the orifice plate is designed to measure the volume flow rate on the compressor curve (Figure 4). Considering the surge cycle is expected at a low volume flow rate, an improvement of the orifice plate should be conducted to utilize it as a valid reference at lower flow rates.

It is important to mention that GUM contains a more mathematical and theoretical approach to the field of uncertainty calculations, where this thesis provides a more practical approach, where the principles of the GUM are applied. Besides, it can be hard to give values for uncertainties with a high level of confidence. Therefore, uncertainties also have uncertainty, such as signal processing and flow calculation, which normally is very small and neglected in the thesis.

### 5.4 Sensitivity analysis results

Figure 20 shows the absolute uncertainty at a high mass flow rate and what contributes to this uncertainty. At a mass flow rate of 1.58 kg/s, the discharge coefficient contributes to 70 % of the total uncertainty, while the DP transmitter stands for 13 %.

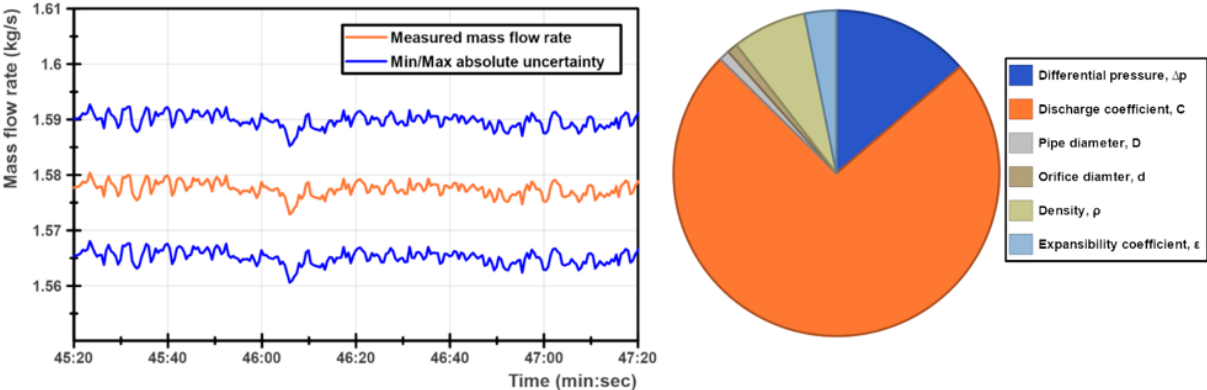


Figure 20 Orifice plate sensitivity analysis result with high mass flow rate

Figure 21 shows the absolute uncertainty at a low mass flow rate and what contributes to this uncertainty. At a mass flow rate of 0.23 kg/s, the discharge coefficient contributes to only 1 % of the total uncertainty, while the DP transmitter stands for 98 %.

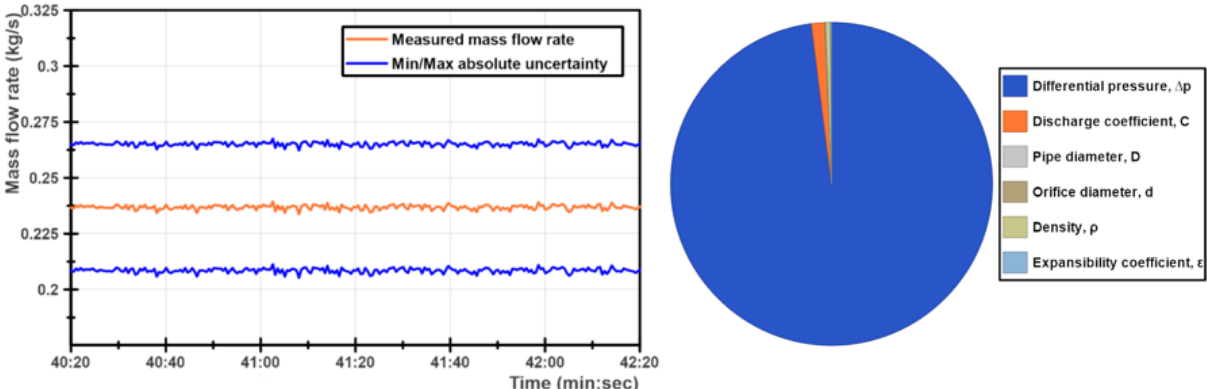


Figure 21 Orifice plate sensitivity analysis result with low mass flow rate

### Summary and conclusion

To be able to make improvements related to the uncertainty of the orifice plate, a sensitivity analysis was utilized. The sensitivity analysis gives additional information to the uncertainty analysis and finds the dominant input parameters that lead to the overall uncertainty of the orifice plate.

The analysis shows that the DP is the dominant parameter at a low mass flow rate, while the discharge coefficient dominates at higher mass flow rates. As the surge cycle is in the lower flow region, attention must be given to the DP transmitter. The use of the word sensitivity analysis in this thesis is a bit misleading. The objective was to present which input parameters contributed the most to uncertainty at different flows with a percentage distribution from equation 5.6. A credible and well-executed analysis has a greater mathematical focus and was not the focus of the thesis [25].

### 5.5 Recommendation to improve the uncertainty

Figure 22 shows the relative expanded uncertainty between the different orifice plates. The smaller plate works like a throttle valve and increases the DP, which gives lower uncertainty. The test shows a significant decrease in uncertainty by changing to a smaller plate, but the measuring range is reduced to cover only up to 0.8 kg/s.

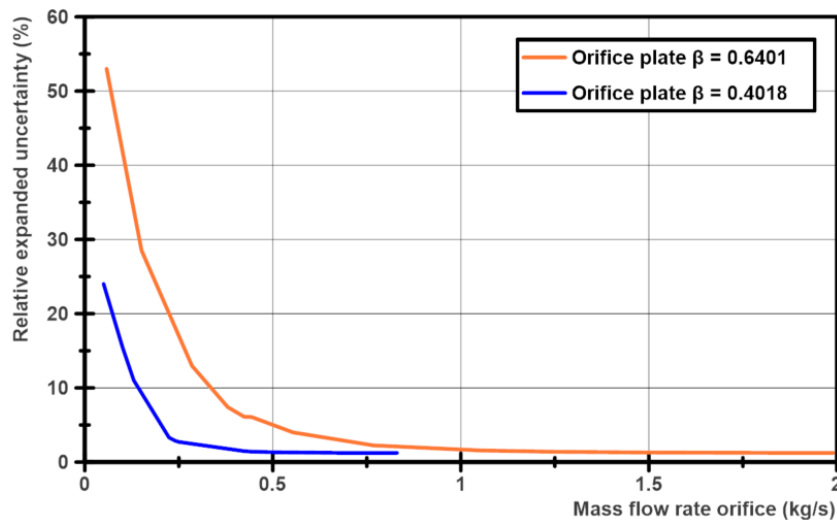
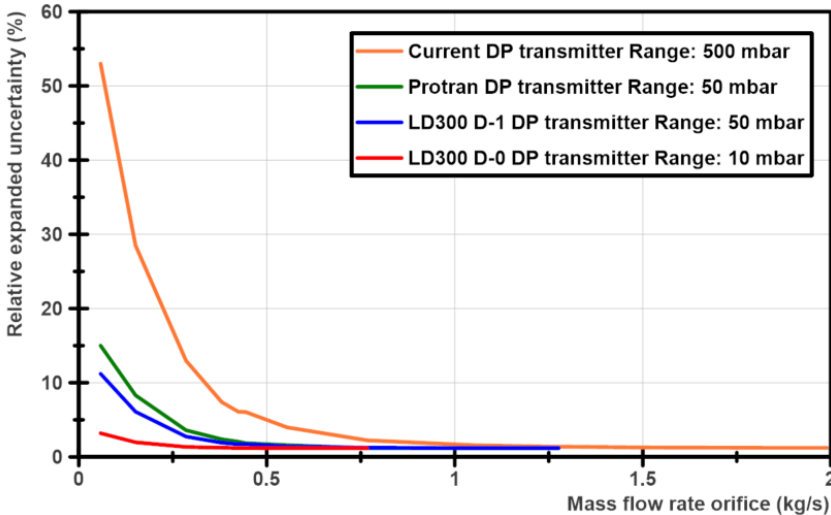


Figure 22 Orifice plate relative expanded uncertainty with different plates

After contacting sellers within DP transmitter, three possible transmitters were recommended. Figure 23 shows the relative expanded uncertainty between the different transmitters. Two of the offers are from the same model (LD300) already installed but intended to measure at a lower flow rate. The Protran transmitter has other technical specifications than models given by LD300. The complete uncertainty analysis for each transmitter is listed in Appendix D.



**Figure 23 Orifice plate relative expanded uncertainty with different DP transmitters**

Figure 24 shows the effect of a 2.4 m longer pipe upstream and the thermometer placed 0.5 m longer upstream. This leads to eliminating the added 0.5 % uncertainty on the discharge coefficient. The relative expanded uncertainty would then decrease to 0.84 % at a mass flow rate over 1.75 kg/s.

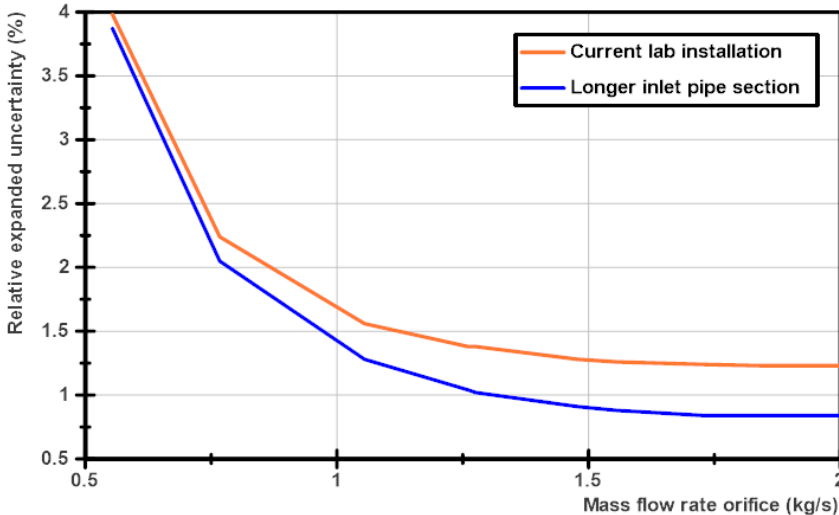


**Figure 24 Orifice plate relative expanded uncertainty with longer inlet pipe section**

### *Summary and conclusion*

Changing the current orifice plate design is necessary to conduct accurate measurements at low flow rates. A thorough assessment of the various alternatives lays the foundation for being able to decide the appropriate solutions.

The test shows that changing the orifice plate ( $\beta = 0.4018$ ) is a good solution to decrease the uncertainty at low flow rates. This solution is free and requires only a proper installation.

Buying a new DP transmitter will also lower the uncertainty significantly, but this solution will cost money. LD300 D-0 transmitter lowers the uncertainty the most, but other aspects of the transmitter must also be studied related to surge (resolution, response time, max working pressure) measurements.

Since the DP transmitter accounts for a large part of the uncertainty, it could have been possible to calibrate the transmitters with a valid certificate. Thus, the accuracy and stability in the uncertainty budget (Table 5) would be lowered. However, this would require certificate equipment or execution of an approved calibration institution. Another solution that could reduce the uncertainty is to use more than one DP transmitter at the orifice plate. The standard uncertainty of the DP transmitter would then be reduced with  $1/\sqrt{X}$  ( $X$  = number of transmitters), as compared to only one transmitter. A change in pipe layout would then be necessary and is not prioritized. Since a significant part of flow measuring in the test facility is on the compressor curve at a higher flow rate, Figures 21 and 24 are included, where an uncertainty below 1 % is defined as good [10].



## 6 Experimental results and analysis

This chapter summarizes the work related to giving reliable flow measurements during the investigation of the surge cycle. The topics presented here include a pressure test, new test facility setup, venturi meter validation, and a surge case.

### 6.1 Pressure test

To utilize the venturi meter during the surge cycle research, establishing a reliable validation (against the orifice plate) and a DP transmitter performance test is necessary. This section analyses the orifice plate and venturi meters DP transmitter with a pressure test. The pressure tests were conducted utilizing an air compressor blowing air into a T piece, with equal cable length connected directly on the DP transmitters' high-pressure side, shown in Figure 25.

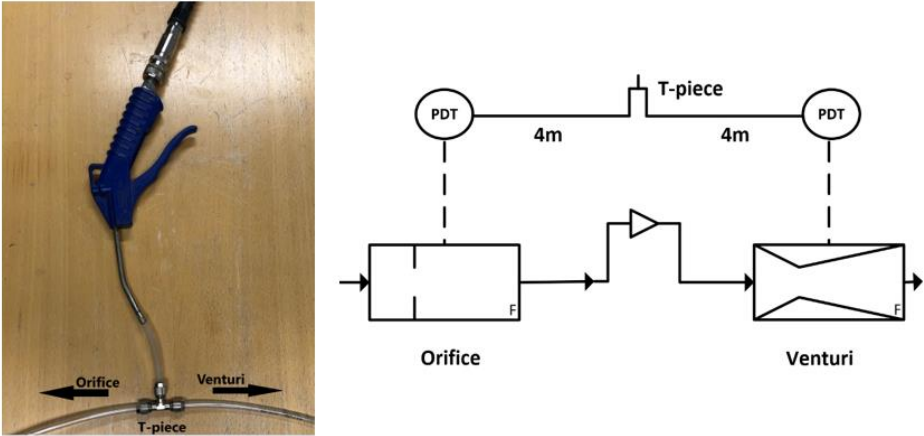


Figure 25 Pressure test setup

Based on ten pressure tests, an average output signal delay of 160 ms on the orifice plate DP transmitter compared to the venturi meter was detected, shown in Figure 26. An offset correction during transient venturi meter validation is thus necessary, shown in Figure 27. A total response time of 100 ms is given in the datasheet, while the test shows a total response time of nearly 400 ms.

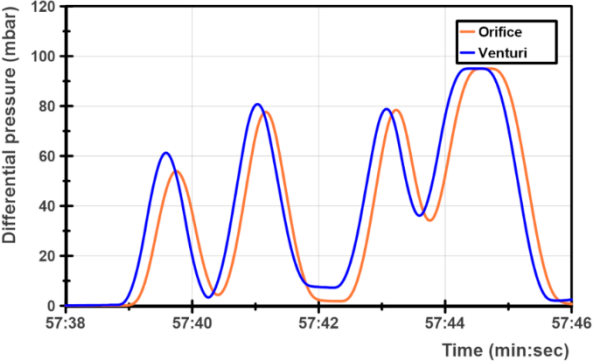


Figure 26 Signal delay

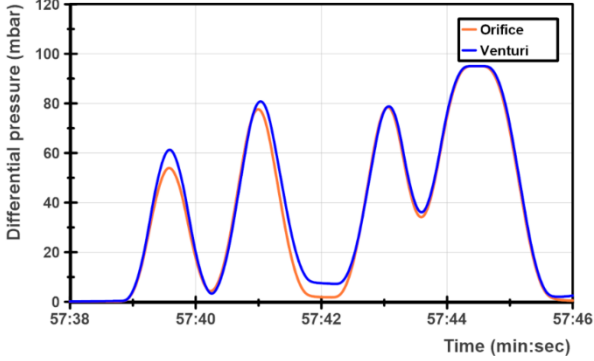


Figure 27 Signal correction

### *Summary and conclusion*

Correct and fast enough output signal on the DP transmitters is a prerequisite to validate the venturi meter and determine if it is suitable for detecting surge cycle in the test facility.

The pressure test detected an output delay on the orifice plates DP transmitter compared to the venturi meter and a slow response time on both transmitters. A slow pressure response will lead to a low pass filtered signal. Possible reasons for the signal delay may be due to the age difference of the DP transmitters or the rig setup (cable length, mounting angle, transmitter damage). In principle, the DP measurement should give equal value, an improvement of the pressure test setup should be considered. Recommendations for improvements are shorter cable length and a more stable pressure source.

## 6.2 New test facility setup

A correct choice of DP transmitter is essential to give reliable flow measurement under investigating the surge cycle in the test facility. Based on the uncertainty analysis, the pressure test, transmitter specification, and the test facility operation area, it has been decided to purchase new DP transmitters for both the orifice plate and the venturi meter.

**Table 11 DP transmitter evaluation**

	Protran PR3202	LD300 D-2	LD300 D-1	LD300-0
Accuracy	OK	Bad	OK	Good
Response time	Good	Bad	Bad	Bad
Max working pressure	OK	Good	OK	Bad
Resolution	OK	OK	OK	OK

**Table 12 New DP transmitters**

Transmitter	Range
Orifice plate	±25 mbar
Venturi PDT1	±10 mbar
Venturi PDT2	±10 mbar

Protran transmitter was selected based on a significantly lower response time (1 ms) compared to the LD300 D-1. As a result, three new Protran DP transmitters were purchased, with the range adjusted for their purpose, shown in Table 12.

Remarks should nevertheless be taken as the stated Protran response time is given from 10-90 % output signal and not the total response time. However, this should provide significantly better accuracy and response time during surge cycle investigation.

It is worth mentioning that the NTNU compressor test facility is instrumented with transmitters more accurately than those found in a standard compressor facility. A standard compressor facility is designed for safety and control and will not be sufficient for detailed transient analyses. However, current research is highly dependent on test data from real-scale compressor rigs, such as the compressor test facility built at the NTNU. It thus provides a unique opportunity to explore different operation scenarios that are not possible in a standard compressor facility.

Figure 28 shows the relative expanded uncertainty effects of the new DP transmitter on the orifice plate combined with changing the plate size. A new LD300 D-2 transmitter with a range of 500 mbar was also purchased for the orifice plate, with the intention of equalizing the signal delay between the orifice plate and venturi meters output signal.

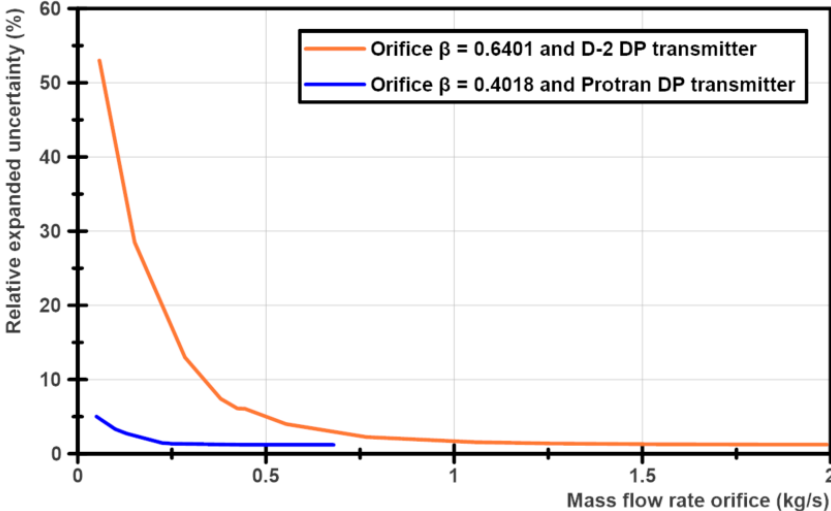


**Figure 28 Orifice plate relative expanded uncertainty for current and new setup**

The new DP transmitters will be delivered after submission of the thesis, and the orifice plate is  $\beta = 0.6401$  as another student needs to take advantage of the entire compressor curve. Thus, the current setup is the basis for further investigation in this thesis.

### 6.3 Validation of venturi meter

Establishing accurate and reliable venturi meter measurement is paramount, as it forms a necessary basis for investigating the surge cycle in the test facility. This section analyses the venturi meter accuracy for normal and reverse flow by utilizing the orifice plate as a reliable reference. The focus is on steady-state measurements, but as surge is a highly transient appearance, a transient validation is conducted to see if it correlates with the steady-state measurements.

#### Steady-state venturi meter validation

Figure 29 shows the venturi meter measuring deviation compared to the reliable orifice plate under steady-state measurements with normal flow. The different steady-state validation points (marked square) were established by utilizing the compressor speed and discharge throttle valve to regulate the orifice mass flow rate. It can be seen that the venturi meter measures too much to about 0.4 kg/s, but above this point, the venturi meter measures too small with an approximately linear deviation in relation to the orifice mass flow rate. The relative deviation between the orifice plate and the venturi meter is in the range of  $\pm 2.5\%$ .

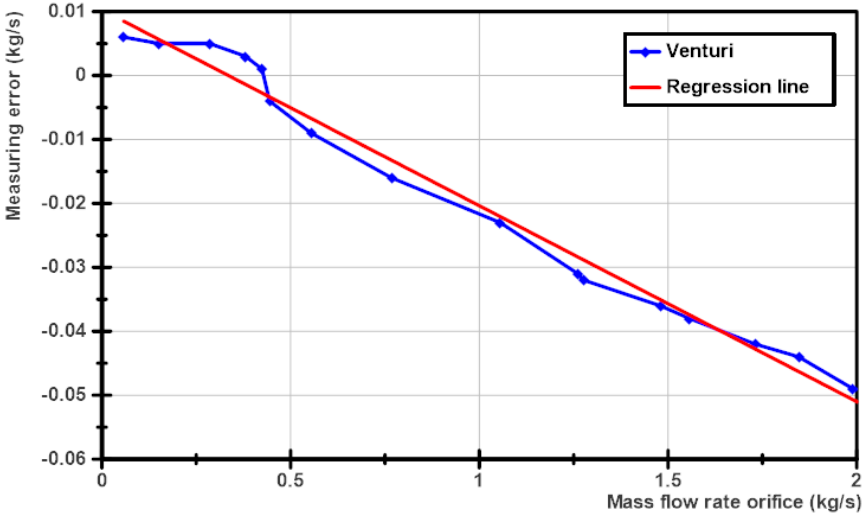
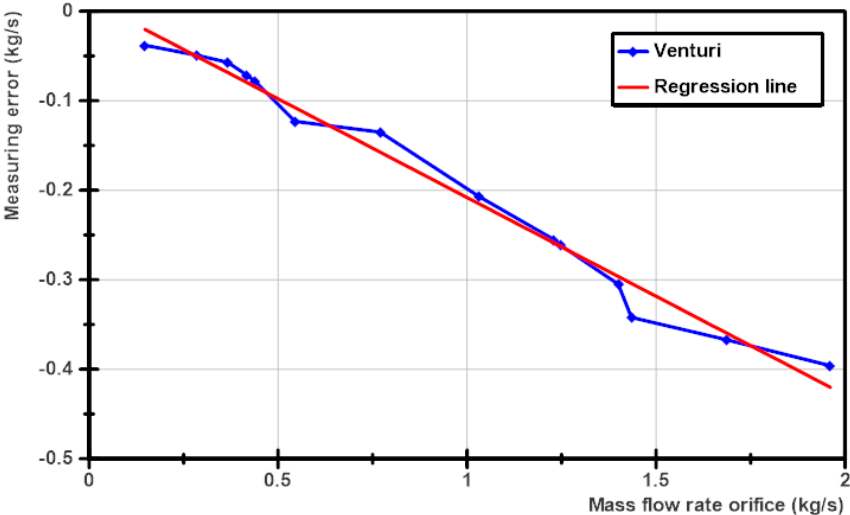


Figure 29 Steady-state venturi meter validation under normal flow

Based on the test a correction factor for the venturi meter mass flow rate at normal flow direction has been established (Regression line):

$$massflow = -0.010 + (0.031 \cdot measured\ massflow) + measured\ massflow \quad (6.1)$$

Since the venturi meter is portable, it was turned 180° with the divergent section in front to validate reverse flow measurement. Figure 30 shows the venturi meter measuring deviation compared to the reliable orifice plate under steady-state measurements with reverse flow. The test shows that the venturi meter measures with a significant deviation under reverse flow, where the relative deviation between the orifice plate and the venturi meter mass flow rate is approximately 20 %.



**Figure 30 Steady-state venturi meter validation under reverse flow**

Based on the test a correction factor for the venturi meter mass flow rate at reverse flow direction has been established (Regression line):

$$massflow = 0.012 + (0.221 \cdot measured\ massflow) + measured\ massflow \quad (6.2)$$

*Transient venturi meter validation*

As surge is a highly transient phenomenon, a transient venturi meter validation is necessary for normal and reverse flow. Two different scenarios were investigated. Table 13 and 14 shows the test matrices for the two scenarios. The purpose of the high mass flow rate test was to see if these coincide with the steady-state measurement and build credibility to the correction factor, although the focus must be directed to low mass flow rate validation.

**Table 13 Test conditions - Transient - Low flow**

Parameter	Quantity
Compressor speed	2000 RPM
Discharge throttle valve	100 % → 40 % → 100 %
Hold time/Rise time	4 s/2 s

**Table 14 Test conditions - Transient - High flow**

Parameter	Quantity
Compressor speed	9000 RPM
Discharge throttle valve	100 % → 40 % → 100 %
Hold time/Rise time	4 s/2 s

Figure 31 and 32 shows the transient test at a low flow rate. At normal flow direction, there is a negligible difference between the orifice plate and the venturi meter. Under reverse flow, a significant venturi meter measurement deviation occurs, equivalent to the steady-state validation.

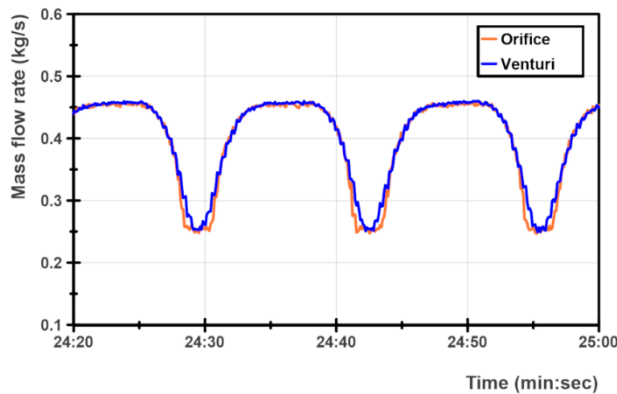


**Figure 31 Transient validation normal low flow**

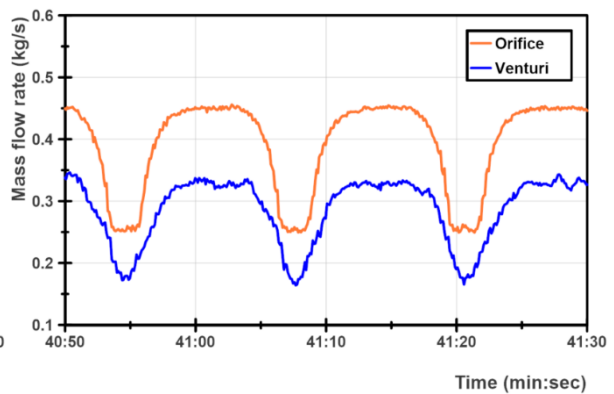


**Figure 32 Transient validation reverse low flow**

Figure 33 and 34 shows the transient test at a high flow rate. The test shows that measurements with reversing flow become more unstable than at low mass flow rate. Otherwise, they indicate the same.

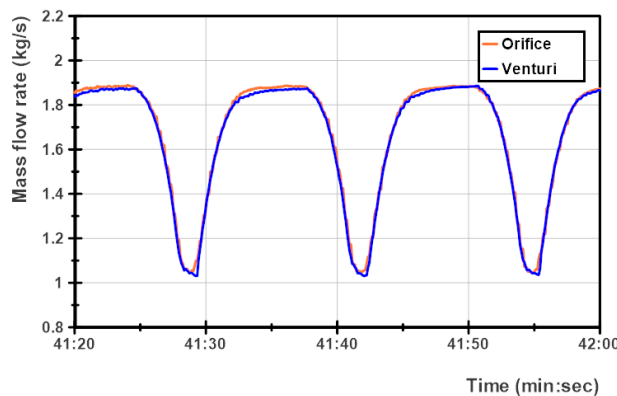


**Figure 33 Transient validation normal high flow**

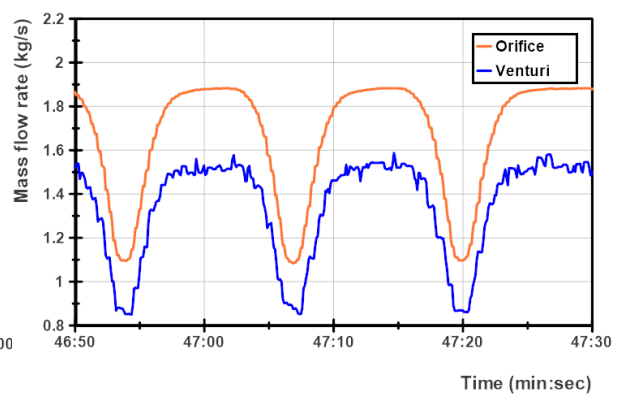


**Figure 34 Transient validation reverse high flow**

### *Summary and conclusion*

Accurate venturi meter measurement is the basis for reliable surge cycle measurement in the test facility. How reverse flow affects the test facilities venturi meter is of particular interest. A comparison of the measured mass flow rate between the reliable orifice plate and venturi meter for normal and reverse flow was made to determine the measurement deviation.

The test reveals only a small measurement deviation at normal flow, while the venturi meter measures a significant deviation at reverse flow under steady-state and transient measurement validation. Thus, the test shows the importance of a correction in the venturi meter by reversing flow to obtain correct measurements during an examination of the surge cycle.

A more comprehensive transient validation should be performed, but the test indicates a good correlation with the steady-state validation. The correction factor established for steady-state normal and reverse flow can thus also be used during transient surge cycle investigation. The uncertainty analysis documented that the relative expanded uncertainty to the reference orifice plate at a low mass flow rate is high. Thus, there is also more significant uncertainty associated with the validation of the venturi meter at a low mass flow rate.



## 6.4 Surge case

The current section investigates the surge cycle based on the current test facility instrumentation, uncertainty analysis, and venturi meter validation. This section describes how to determine if there is normal or reverse flow in the venturi meter and investigate the flow measurement under compressor surge.

### Calculation

An orifice plate design will give a negative DP value in reverse flow, while a venturi meter should in principle always give positive DP values [\(3.1 Principle\)](#) regardless of flow direction. Understanding whether there is normal or reversed flow in the venturi meter is a prerequisite for analyzing the surge cycle. Using the DP transmitter 2 (Figure 17) can determine the flow direction, where a positive or negative pressure loss (Figure 9) over the venturi meter indicates the direction. The pressure loss will be significantly higher during reverse flow due to the venturi meter design.

$$Flow\ direction = \frac{\sqrt{(DPT2)^2}}{DPT2} \quad (6.3)$$

$$1 = Normal\ flow \quad -1 = Reverse\ flow$$

Using this in equation 4.10:

$$\dot{m} = \frac{C}{\sqrt{1-\beta^4}} \varepsilon \frac{\pi}{4} d^2 \sqrt{2\Delta p \rho_1} \cdot Flow\ direction \quad (6.4)$$

The pressure loss over the venturi meter in the test facility is very low at normal flow and a bit higher at reverse flow. Thus, the DP transmitter has to have great performance at low flows and handle a higher `max working pressure`. The Protran transmitter with a range of  $\pm 10$  mbar was purchased for this purpose. Test of the venturi meter compared to the orifice plate shows a good correlation on flow direction, but further tests with the new transmitter have to be conducted to validate flow direction by utilizing the pressure loss.

## Test

In order to be sure that the compressor operates in the surge area and provides reverse flow, the pressure tank was utilized. By utilizing the pressure tank, the orifice plate also experiences reverse flow, which certainly gives a reversing flow in the venturi meter and provides credibility to the detection of flow direction. Table 15 shows the test matrices for the experiment.

**Table 15 Test condition - Surge case**

Parameter	Quantity
Compressor speed	9000 RPM
Discharge throttle valve	30 %
Pressure tank	3.2 bar → 0 bar

Figure 35 shows the initiation of the experiment. The compressor operates far up the compressor curve towards the surge line when the manual pressure tank valve was opened. A distinct drop in compressor speed confirms that the pressure enters the compressor, and flow oscillation through the compressor is provoked before the VSD starts recovering the speed. Simultaneously the DP at the venturi meter gives a constant negative value in 2.5 seconds.

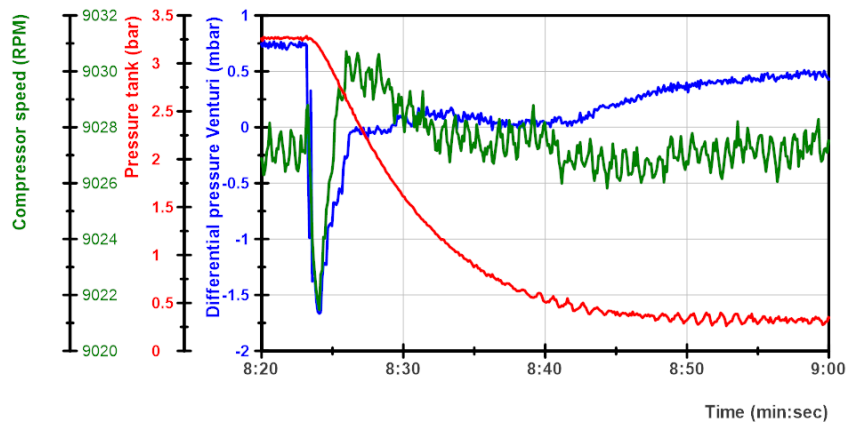


**Figure 35 Surge case**

As a negative DP on the venturi meter in principle never should happen, it is uncertain about the flow in the venturi meter. A DP value of zero is expected when the flow direction is just about to change direction, and never a longer negative DP value. In consultation with the supervisor, it was decided to stop a further investigation of the surge cycle in this thesis.

### *Summary and conclusion*

The surge cycle represents a serious concern for a centrifugal compressor. It is vital to have reliable flow measurements to detect the surge cycle, distinguishing between normal and reverse flow. An experimental test was conducted to attempt to analyze the surge cycle utilizing the venturi meter.

Utilizing the pressure loss over the venturi meter works to decide the flow direction, given that the DP transmitter is customized. Further investigation is necessary to validate the venturi flow direction. Possible solutions are to place treads inside the venturi meter to validate the flow direction in conjunction with the pressure loss. Another solution may be to use the suction pressure the compressor creates. As the DP at the venturi meter gives a negative value under the test, there is difficult to give reliable flow measurements, and further investigation has to be conducted. The test shows how vital reliable flow measurements are when analyzing the surge cycle.

## 7 Conclusion and recommendations for further work

### 7.1 Conclusion

Based on an evaluation of the NTNU compressor test facility, the main objective was to discover and document if it was appropriate to detect an accurate and reliable surge cycle. The following list presents the most important discoveries in this thesis:

- Reliable flow measurement is vital to investigate the surge cycle in a centrifugal compressor, in terms of accuracy, transient, and reverse flow. As the surge cycle gives reverse flow, flow calculation based on standards using DP devices has its limits in low and reverse flow.
- The portable venturi meter is the most appropriate DPM in the NTNU compressor test facility to detect the surge cycle, but a validation of the accuracy against the standard orifice plate is necessary.
- The orifice plate is not suitable for low flow measurement with the current test facility setup. A high relative expanded uncertainty at a low flow rate is detected. A new DP transmitter and a smaller orifice plate are necessary to get better accuracy at a low flow rate and thus improve the venturi validation.
- The present DP transmitter in the venturi meter is not appropriate for surge cycle measurement due to slow response time and poorly fitted range. Based on an overall evaluation, Protran PR3202 with adapted range is the most suitable transmitter for surge cycle research for both the orifice plate and venturi meter.
- Reverse flow in the venturi meter provides a significant measuring error compared to normal flow. A relative deviation of 20 % was measured. A correction factor when measuring reverse flow using a venturi meter is thus necessary during the surge cycle research.
- The surge experiment gives a negative DP value at the venturi meter. The test shows how important reliable flow measurement is when analyzing the surge cycle.

## 7.2 Recommendations for further work

Establishing the accuracy of the venturi meter during normal, transient, and reverse flow with the new Protran transmitter is a good starting point when investigating the surge cycle in the test facility. This requires a better reference orifice plate. The following steps are recommended:

- Change the plate size to  $\beta = 0.4018$  and install the new Protran transmitter on the orifice plate.
- Install new DP transmitter on the venturi meter, both DPT1, and DPT2.
- Pressure test to validate the response time and signal delay between the orifice plate and venturi meter DP.
- Validation of the venturi meter. Investigate solutions to place the orifice plate and venturi meter close to each other and perform a reliable transient validation.
- A more comprehensive test that determines the direction of flow in the venturi meter. Possible solutions are to use threads inside the venturi meter in combination with a high speed-camera connected against the measurements system.
- More studies are necessary for a deeper surge cycle analysis based on the findings related to negative DP in the venturi meter.

## 8 References

- [1] S. Dixon and C. Hall, *Fluid Mechanics and Thermodynamics of Turbomachinery*, Elsevier, 2014.
- [2] J. M. Shultz, "The Polyropic Analysis of Centrifugal Compressors," *Journal of Engineering for Power*, 1962.
- [3] S. Ueland, "Digital compressor modelling," NTNU, 2021.
- [4] K. Brun, S. Simons, R. Kurz, E. Munari, M. Morini and M. Pinelli, "Measurement and prediction of centrifugal compressor axial forces during surge-part 1: Surge force measurements," *Journal of engineering for gas turbines and power*, GTP-17-1223, ASME, 2017.
- [5] G. K. McMillan, *Centrifugal and axial compressor control*, Momentum Press, 2010.
- [6] G. N. Boum, R. Bontempo and I. Trebinjac, "Three-Dimensional/One-Dimensional combined simulation of deep surge loop in a turbocharger compressor with vaned diffuser," *Journal of engineering for gas turbines and power*, GTP-18-1647, ASME, 2019.
- [7] F. Zhao, J. Dodds and M. Vahdati, "Flow physics during surge and recovery of a multi-stage high speed compressor," *ASME Turbo Expo 2020: Turbomachinery Technical Conference and Exposition*, GT2020-14345, 2021.
- [8] G. Liskiewicz, M. Kulak, K. Sobczak and M. Stickland, "Numerical model of a deep surge cycle in low-speed centrifugal compressor," *Journal of Turbomachinery*, TURBO-20-1002, ASME, 2020.
- [9] A. Hunter, R. Nyquist and S. Coller, "Orifice flow calculation: Comparison between fluid meter applications- 6th edition 1971, ASME PTC 19.5-2004 and ISO 5167-2003," *ASME 2013 Power Conference*, POWER2013-98268, 2013.
- [10] M. Reader-Harris, *Orifice Plates and Venturi Tubes*, Springer, 2015.
- [11] M. J. Reader-Harris, G. J. Brown, J. J. Gibson and G. J. Stobie, "Correction of readings from an orifice plate installed in reverse orientation," *North sea flow measurement workshop*, 2000.
- [12] M. Alan and R. Langari, *Measurement and Instrumentation*, Academic press, 2012.
- [13] T. G. Gruner and L. E. Bakken, "Wet gas impeller test facility," *ASME Turbo Expo: Power for Land, Sea and Air*, GT2010-22618, 2010.
- [14] NS-EN ISO 5167-2, "Measurement of fluid flow by means of pressure differential devices inserted in circular cross-section conduits running full- Part 2: Orifice plates," *Standard Norge*, 2003.
- [15] ISO/TR 3313, "Measurement of fluid in closed conduits - Guidelines on the effects of flow pulsations on flow-measurement instruments," *Standard Norge*, 2018.

- [16] NS-EN ISO 5167-4, "Measurement of fluid flow by means of pressure differential devices inserted in circular cross-section conduits running full - Part 4: Venturi Tubes," Standard Norge, 2003.
- [17] O. Mehlum, Ø. Hundseid and L. E. Bakken, "Experimental analysis of Venturi-tube behavior in wet gas conditions," ASME International Mechanical Engineering Congress and Exposition, IIMECE2020-23707, 2020.
- [18] S. Gupta, Measurement Uncertainties: Physical parameters and calibration of instruments, Springer, 2012.
- [19] G. Steele and H. Coleman, Experimentation, validation, and uncertainty analysis for engineers, John Wiley and sons, 2009.
- [20] NEK ISO/IEC GUIDE 98-1, "Uncertainty of measurement - Part 1: Introduction to the expression of uncertainty in measurement," Standard Norge, 2009.
- [21] NEK ISO/IEC GUIDE 98-3, "Uncertainty of measurement- Part 3: Guide to the expression of uncertainty in measurement (GUM:1995)," Standard Norge, 2008.
- [22] NEK ISO/IEC GUIDE 98-3-SP1, "Uncertainty of measurement - Part 3: Guide to expression of uncertainty in measurement (GUM:1995) - Propagation of distributions using a Monte Carlo method," Standard Norge, 2008.
- [23] NS-EN ISO 5167-1, "Measurement of fluid flow by means of pressure differential devices inserted in circular cross-section conduits running full," Standard Norge, 2003.
- [24] E. O. Dahl, K.-E. Frøysa, P. Lunde and C. Michelsen, "Handbook of uncertainty," Norwegian society for oil and gas measurement , 2003.
- [25] A. Saltelli, K. Aleksankina, W. Becker, P. Fennel, F. Ferretti, N. Holst, S. Li and Q. Wu, "Why so many published sensitivity analyses are false: A systematic review of sensitivity analysis practices` Environmental Modelling and software 114 p29-39," 2019.

## 9 Appendix



# A Risk assessment

 HSE/KS	Risk assessment	Prepared by	Number	Date	
		HSE section	HMSRV2603E	24.03.2021	
		Approved by		Replaces	
		The Rector		01.12.2006	

Unit: Department of Energy and Process Engineering

Date: 24/3/2021

Line manager: Lars Eirik Bakken

Participants in the identification process: Erlend Randen, Erik Langørgen

Short description of the main activity/main process: Operating compressor |

Is the project work purely theoretical? NO

Responsible supervisor: Erik Langørgen

Student: Erlend Randen

Activity	Potential undesirable incident/strain	Likelihood: (1-5)	Consequence:			Risk Value (human)	Comments/status Suggested measures
			Human (A-E)	Environment (A-E)	Economy/material (A-E)		
Operating compressor	Noise	1	2	1	1	2	Use of hearing protection.
Operating compressor	Flying small parts	1	2	1	1	2	Use of goggles
Operating compressor	Breakdown	1	4	3	2	4	Training and knowledge of where the emergency stop are
Operating compressor	Heat run	1	1	1	3	1	Knowledge of the compressors operating area

Likelihood, e.g.:

1. Minimal
2. Low
3. Medium
4. High
5. Very high

Consequence, e.g.:

- A. Safe
- B. Relatively safe
- C. Dangerous
- D. Critical
- E. Very critical

Risk value (each one to be estimated separately):

Human = Likelihood x Human Consequence

Environmental = Likelihood x Environmental consequence

Financial/material = Likelihood x Consequence for Economy/material

## Potential undesirable incident/strain

Identify possible incidents and conditions that may lead to situations that pose a hazard to people, the environment and any materiel/equipment involved.

## Criteria for the assessment of likelihood and consequence in relation to fieldwork

Each activity is assessed according to a worst-case scenario. Likelihood and consequence are to be assessed separately for each potential undesirable incident. Before starting on the quantification, the participants should agree what they understand by the assessment criteria:

### Likelihood

Minimal 1	Low 2	Medium 3	High 4	Very high 5
Once every 50 years or less	Once every 10 years or less	Once a year or less	Once a month or less	Once a week

### Consequence

Grading	Human	Environment	Financial/material
E Very critical	May produce fatality/ies	Very prolonged, non-reversible damage	Shutdown of work >1 year.
D Critical	Permanent injury, may produce serious health damage/sickness	Prolonged damage. Long recovery time.	Shutdown of work 0.5-1 year.
C Dangerous	Serious personal injury	Minor damage. Long recovery time	Shutdown of work < 1 month
B Relatively safe	Injury that requires medical treatment	Minor damage. Short recovery time	Shutdown of work < 1week
A Safe	Injury that requires first aid	Insignificant damage. Short recovery time	Shutdown of work < 1day

The unit makes its own decision as to whether opting to fill in or not consequences for economy/materiel, for example if the unit is going to use particularly valuable equipment. It is up to the individual unit to choose the assessment criteria for this column.

Risk = Likelihood x Consequence

Please calculate the risk value for "Human", "Environment" and, if chosen, "Economy/materiel", separately.

Figure 36 Risk assessment

## B Datasheets

The complete datasheets are given to the supervisor.

### B.1 LD300 D-2

Technical Characteristics	
LD300 Serie	
Performance Specifications	
<b>Reference Conditions</b>	Span starting at zero, temperature of 25 °C (77 °F), atmospheric pressure, power supply of 24 Vdc, silicone oil fill fluid, isolating diaphragms in 316L SST and digital trim equal to lower and upper range values.
<b>Accuracy</b>	<p><b>For range 0, differential and gage models, diaphragms in SST 316L, fill fluid in Silicone or Halocarbon:</b>  <math>0.1 \text{ URL} \leq \text{span} \leq \text{URL}: \pm 0.2\%</math> of span  <math>0.05 \text{ URL} \leq \text{span} \leq 0.1 \text{ URL}: \pm 0.1 [1 + 0.1 \text{ URL}/\text{span}]</math>% of span</p> <p><b>For ranges 1, 2, 3 and 4:</b>  <math>0.1 \text{ URL} \leq \text{span} \leq \text{URL}: \pm 0.075\%</math> of span  <math>0.025 \text{ URL} \leq \text{span} \leq 0.1 \text{ URL}: \pm 0.0375 [1 + 0.1 \text{ URL}/\text{span}]</math>% of span  <math>0.0085 \text{ URL} \leq \text{span} \leq 0.025 \text{ URL}: \pm [0.0015 + 0.00465 \text{ URL}/\text{span}]</math>% of span</p> <p><b>For ranges 5 and 6, absolute models; diaphragms in Tantalum or Monel; or fill fluid in Fluorolube:</b>  <math>0.1 \text{ URL} \leq \text{span} \leq \text{URL}: \pm 0.1\%</math> of span  <math>0.025 \text{ URL} \leq \text{span} \leq 0.1 \text{ URL}: \pm 0.05 [1 + 0.1 \text{ URL}/\text{span}]</math>% of span  <math>0.0085 \text{ URL} \leq \text{span} \leq 0.025 \text{ URL}: \pm [0.01 + 0.006 \text{ URL}/\text{span}]</math>% of span</p> <p><b>For absolute models, range 1:</b>  <math>\pm 0.2\%</math> of span                      Linearity, hysteresis and repeatability effects are included.</p>
<b>Stability</b>	$\pm 0.4\%$ of URL for 12 months for range 0, at 20 °C temperature change and up to 100 kPa (1 bar) of static pressure $\pm 0.1\%$ of URL for 24 months for ranges 2, 3, 4, 5 & 6 $\pm 0.2\%$ of URL for 12 months for range 1 & L models $\pm 0.25\%$ of URL for 5 years, at 20 °C temperature change and up to 7 MPa (1000 psi) of static pressure
<b>Temperature Effect</b>	$\pm (0.1\% \text{ URL} + 0.3\% \text{ span})$ per 20 °C for range 0 $\pm (0.02\% \text{ URL} + 0.1\% \text{ span})$ per 20 °C (36 °F) for ranges 2, 3, 4, 5 & 6 $\pm (0.05\% \text{ URL} + 0.15\% \text{ span})$ per 20 °C (36 °F) for range 1 For LD300L: 6 mmH <sub>2</sub> O per 20 °C for 4" and DN100 17 mmH <sub>2</sub> O per 20 °C for 3" and DN80 Consult for other flange dimensions and fill fluid.
<b>Static Pressure Effect</b>	<p><b>Zero error:</b>  <math>\pm 0.1\%</math> URL per 7 MPa (1000 psi) for ranges 2, 3, 4 &amp; 5  <math>\pm 0.1\%</math> URL per 3.5 MPa (500 psi) for L models  <math>\pm 0.1\%</math> URL per 1.7 MPa (250 psi) for range 1  <math>\pm 0.2\%</math> URL per 0.5 MPa (5 bar) for range 0                      The zero error is a systematic error that can be eliminated by calibrating at the operating static pressure.</p> <p><b>Span error:</b>                      Correctable to <math>\pm 0.2\%</math> of reading per 7 MPa (1000 psi) for ranges 2, 3, 4 &amp; 5 or 3.5 MPa (500 psi) for range 1 and L models.                      Correctable for <math>\pm 0.2\%</math> of reading per 0.5 MPa (5 bar) for range 0.</p>
<b>Power Supply Effect</b>	$\pm 0.005\%$ of calibrated span per volt
<b>Mounting Position Effect</b>	Zero shift of up to 250 Pa (1 inH <sub>2</sub> O) which can be calibrated out. No span effect.
<b>Electro-Magnetic Interference Effect</b>	Approved according to IEC 61000-6-2, IEC 61000-6-4 and IEC 61326:2002.

Figure 37 Datasheet - LD300 D-2

## B.2 PCE-28



ALW type



ALM type

### ALW and ALM type

Aluminum casing with programmable local display. The design of the casing enables the use of a local display, rotation of the display, rotation of the casing by 0–345° relative to the sensor. Electrical connection DIN EN 175301-803, IP65 (special version with cable electrical connection and IP67).

Display with backlight allows to read:  
 - measured pressure in user units or % of measuring range  
 - current in output loop in mA

### Application and construction

The PCE-28 pressure transmitter is applicable to the measurement of the pressure, underpressure and absolute pressure of gases, vapours and liquids. The active sensing element is a piezoresistant silicon sensor separated from the medium by a diaphragm and by specially selected type of manometric liquid. The electronics is placed in a casing with a degree of protection from IP 65 to IP 68, depending on the type of electrical connection applied.

### Calibration

Potentiometers can be used to shift the zero position and the range by up to ±10%, without altering the settings (not possible with ALM and SG casing).

### Installation

The transmitter is not heavy, so it can be installed directly on the installation. When the pressure of steam or other hot media is measured, a siphon or impulse line should be used. The needle valve placed upstream the transmitter simplifies installation process and enables the zero point adjustment or the transmitter replacement.

When the special process connections are required for the measurement of levels and pressures (e.g. at food and chemical industries), the transmitter is provided with an Aplisens diaphragm seal. Installing accessories and a full scope of diaphragm seals are described in detail in the further part of the catalogue.

### Measurements under explosion hazard

ATEX Intrinsic safety version is available for taking measurements in zones under explosion hazard. The installation of the transmitter in a zone under explosion hazard requires the use of a Ex power supply. We recommend the use of the Aplisens ZS-30/1Ex power supply and separator.

### Technical data

**Any measuring range** 0...25 mbar + 0...1000 bar (over pressure, under pressure); 400 mbar + 80 bar (absolute pressure)  
 Measurement of lower pressure ranges, possible using transmitter PRE-50G with GP process connection.

	Measuring range				
	25 mbar	100 mbar	400 mbar	0...1 bar + 160bar	0...160 bar + 1000bar
Overpressure Limit (repeated, without hysteresis)	1 bar	1 bar	2,5 bar	4 x range	2 x range; max. 1200 bar
Damaging Overpressure	2 bar	2 bar	5 bar	8 x range; max. 2000 bar	
Accuracy	0,6%	0,3%	0,2% (0,16% - special version)		
Long term stability	0,6% / year	0,2% / year	0,1% / year		
Thermal error	Typically 0,5% / 10°C Max 0,6% / 10°C	Typically 0,3% / 10°C Max 0,4% / 10°C	Typically 0,2% / 10°C Max 0,3% / 10°C		

<b>Hysteresis, repeatability</b>	0,05%	<b>Output signal</b>	4...20 mA, two wire transmission
<b>Response time</b>	< 120 ms		0...10V
	version TR: < 30 ms	<b>Material of wetted parts</b>	316Lss, Hastelloy C 276, Au
<b>Thermal compensation range</b>	-10...80°C	<b>Material of casing</b>	304ss, 316Lss
<b>Operating temperature range (ambient temp.)</b>	-40...80°C	<b>Power supply</b>	output 4...20mA
<b>Medium temperature range</b>	-40...130°C		8...36 V DC (Ex 9...28 V DC)
over 130°C – measurement with use an impulse line or diaphragm seals			version TR, version Safety: 10,5...36 V DC (Ex 12...28 V DC)
CAUTION: the medium must not be allowed to freeze in the impulse line or close to the process connection of the transmitter			ALW and ALM version: (11...36V DC)
			output 0...10V
			13...30 VDC
		<b>Error due to supply voltage changes</b>	0,005% / V
		<b>Load resistance</b>	$R(\Omega) \leq \frac{U_{sup}[V] - 8V}{0,02A}$

Figure 38 Datasheet - PCE-28

## B.3 CTP5000/CTR5000

Specifications	Model CTP5000-200
<b>Specific probe data <sup>1)</sup></b>	
Temperature range	-50 ... +200 °C [-58 ... +392 °F]
Resistance at 0 °C [32 °F]	100 Ω
Temperature coefficient	0.00385
R(Ga)/R(TPW)	Ratio less than 1.11807
Annual drift <sup>2)</sup>	±10 ... ±20 mK
Recommended measurement current	0.5 mA or 1 mA
Self heating error in water at 0 °C [32 °F]	2 ... 5 mK
Sheath material	Stainless steel
<b>Dimensions</b>	
Probe diameter	d = 3 mm [0.12 in]
Probe length	l = 30 mm [1.18 in], fully immersible
<b>Cable</b>	
Length	3 m [9.84 ft]
Connection	Bare wire, DIN plug or SMART connector

1) Specifications may deviate; they depend on the use of the thermometer. The specified values are typical values for use in laboratories.

2) Previous ageing is required. Recommendation =  $T_{max} + 10$  K over 20 h

## Specifications Model CTR5000

Hand-held thermometer	
Probe types	Industrial platinum resistance thermometers (PRTs) and standard platinum resistance thermometers (SPRTs) with $R_0 = 25 \Omega$ and $100 \Omega$ up to an alpha of 0.00392
Measuring inputs	2 (front panel), 4 or 6 (rear panel) Expandable up to an additional 64 channels with CTS5000 multiplexers
Data entry format	ITS 90 and CVD for calibrated probes; or EN 60751 for uncalibrated probes Optional: coefficient generation from data pairs
<b>Measuring ranges</b>	
Probe current	1 mA (Pt100); optional auto-select 1 mA, 2 mA
Temperature range	-200 ... +962 °C, depending on thermometer probe
Accuracy <sup>1)</sup>	0.01 K, optional 0.005 K

1) The accuracy in K defines the deviation between the measured value and the reference value. (Only valid for indicating instruments.)

Figure 39 Datasheet - CTP5000/CTR5000

## B.4 LD300 D-1 and LD300 D-0

Performance Specifications	
<b>Reference Conditions</b>	Span starting at zero, temperature of 25°C (77°F), atmospheric pressure, power supply of 24 Vcc, silicone oil fill fluid, isolating diaphragms in 316L SST and digital trim equal to lower and upper range values.
<b>Accuracy</b>	<p>For range 0, and differential or gage models and 316L SST or hastelloy diaphragm with silicon or halocarbon filling fluid:</p> <p>0.2 URL ≤ span ≤ URL: ± 0.1% of span            0.05 URL ≤ span &lt; 0.2 URL: ± [0.025+0.015 URL/span]% of span</p> <p>For ranges 1, 2, 3, 4, 5 or 6, differential or gage models, and 316L SST or hastelloy diaphragm with silicon or halocarbon filling fluid:</p> <p>0.1 URL ≤ span ≤ URL: ± 0.075% of span            0.025 URL ≤ span &lt; 0.1 URL: ± [0.0375+0.00375.URL/span]% of span            0.0083 URL ≤ span &lt; 0.025 URL: ± [0.0015+0.00465.URL/span]% of span</p>

6.4

### Technical Characteristics

Performance Specifications	
	<p>For ranges 2 to 6 and absolute model. For tantalum or monel diaphragm. For fluorolube filling fluid:</p> <p>0.1 URL ≤ span ≤ URL: ± 0.1% of span            0.025 URL ≤ span &lt; 0.1 URL: ± 0.05[1+0.1 URL/span]% of span            0.0083 URL ≤ span &lt; 0.025 URL: ± [0.01+0.006 URL/span]% of span</p> <p>For range 1 and absolute model:            ± 0.2% of span</p> <p>For ranges 2, 3 or 4 and level model and 316L SST diaphragm with silicon or halocarbon filling fluid with maximum pressure matching the flange pressure class:</p> <p>0.1 URL ≤ span ≤ URL: ± 0.075% of span            0.025 URL ≤ span &lt; 0.1 URL: ± [0.0375+0.00375.URL/span]% of span            0.0083 URL ≤ span &lt; 0.025 URL: ± [0.0015+0.00465.URL/span]% of span</p> <p>Linearity effects, hysteresis and repeatability are included.</p>
<b>Stability</b>	<p>For ranges 2, 3, 4, 5 and 6: ± 0.15% of URL for 5 years at 20 °C temperature change and up to 7 MPa (1000 psi) of static pressure.</p> <p>For ranges 0 and 1: ± 0.2% of URL for 12 months at 20 °C temperature change and up to 100 kPa (1bar) of static pressure.</p> <p>For Level model: ± 0.2% of URL for 12 months at 20 °C temperature change.</p>
<b>Temperature Effect</b>	<p>For ranges 2, 3, 4 and 5:</p> <p>0.2 URL ≤ span ≤ URL: ± [0.02% URL + 0.06% span] per 20 °C (68 °F)            0.0085 URL ≤ span &lt; 0.2 URL: ± [0.023% URL + 0.045% span] per 20 °C (68°F)</p> <p>For range 1:</p> <p>0.2 URL ≤ span ≤ URL: ± [0.08% URL + 0.05% span] per 20 °C (68 °F)            0.025 URL ≤ span &lt; 0.2 URL: ± [0.06% URL + 0.15% span] per 20 °C (68 °F)</p> <p>For range 0:</p> <p>0.2 URL ≤ span ≤ URL: ± [0.15% URL + 0.05% span] per 20 °C (68 °F)            0.05 URL ≤ span &lt; 0.2 URL: ± [0.1% URL + 0.3% span] per 20 °C (68 °F)</p> <p>For level model:            6 mmH<sub>2</sub>O per 20 °C for 4" and DN100            17 mmH<sub>2</sub>O per 20 °C for 3" and DN80            Consult Smar for other flange dimensions and fill fluid.</p>
<b>Static Pressure Effect</b>	<p><b>Zero error:</b>            For ranges 2, 3, 4 and 5: ± 0.033% of URL per 7MPa (1000 psi)            For range 1: ± 0.05% of URL per 1.7 MPa (250 psi)            For range 0: ± 0.1% of URL per 0.5 MPa (5 bar)            For Level model: ± 0.1% of URL per 3.5 MPa (500 psi)</p> <p>The zero error is a systematic error that can be eliminated by calibrating at the operating static pressure.</p> <p><b>Span error:</b>            For ranges 2, 3, 4, 5 and 6: correctable to ± 0.2% of reading per 7MPa (1000 psi)            For range 1 and level transmitters: correctable to ± 0.2% of reading per 3.5 MPa (500 psi)            For range 0: correctable to ± 0.2% of reading per 0.5 MPa (5 bar) (70 psi)</p>

Figure 40 Datasheet - LD300 D-1 and LD300 D-0

## B.5 Protran PR3202

### Protran® PR3202 Low Pressure Differential Transmitter




#### Technical Data

Type:	PR3202	PR3203	PR3204
Sensor Technology:	Piezoresistive Silicon		
Output Signal:	4-20 mA (2 wire)	0-5 V (3 wire)	0-10 V (3 wire)
Supply Voltage:	10-36 VDC	13 – 30 VDC	13 – 30 VDC
Pressure Reference:	Differential		
Protection of Supply Voltage:	Protected against supply voltage reversal up to 50 V		
Standard Pressure Ranges (bar):	0-5 mbar; 0-10 mbar; 0-20 mbar; 0-50 mbar; 0-100 mbar; 0-250 mbar; 0-500 mbar; 0-1,000 mbar (other options available)		
Standard Pressure Ranges (psi):	0-2 inH <sub>2</sub> O; 0-4 inH <sub>2</sub> O; 0-8 inH <sub>2</sub> O; 0-10 inH <sub>2</sub> O; 0-12 inH <sub>2</sub> O; 0-20 inH <sub>2</sub> O; 0-1 psi; 0-1.5 psi; 0-3 psi; 0-4 psi; 0-7.5 psi; 0-15 psi (other options available)		
Overpressure Safety:	25 mbar max. for ranges 0-5 mbar to 0-10 mbar; 200 mbar max. for ranges 0-20 mbar to 0-100 mbar; 1,200 mbar max. for ranges 0-150 mbar to 0-1,000 mbar		
Common Mode (Static line pressure):	375 mbar equal to both ports for ranges 0-5 to 0-10 mbar; 2 bar max. equal to both ports for ranges 0-20 mbar to 0-1,000 mbar		
Load Driving Capability:	4-20 mA: RL < [UB - 13 V] / 20 mA (e.g. with supply voltage (UB) of 36 V, max. load (RL) is 1150 Ω)		
Accuracy NLHR:	≤ ±0.3 % of span BFSL		
Zero Offset and Span Tolerance:	±1.0% FS at room temperature ±5% FS (approx.) adjustment via trimming potentiometers located beneath the enclosure lid		
Operating Ambient Temperature:	-20 °C to +70 °C (-4 °F to +158 °F)		
Operating Media Temperature:	-20 °C to +70 °C (-4 °F to +158 °F)		
Storage Temperature:	+5 °C to +40 °C (+41 °F to +104°F) Recommended Best Practice		
Temperature Effects:	±2.0% FS total error band for -20 °C to +70 °C. Typical thermal zero and span coefficients ±0.04% FS/ °C		
ATEX/IECEx Approval Option (4-20 mA version only):	Ex II 1 G Ex ia IIC T4 Ga (zone 0) Ex II 1 D Ex ia IIIC T135 °C Da (zone 20) Ex I M 1 Ex ia I Ma (group 1 M1)		N/A
ATEX/IECEx Safety Values:	U <sub>i</sub> = 28 V I <sub>i</sub> = 119 mA P <sub>i</sub> = 0.65 W L <sub>i</sub> = 0.1 μH C <sub>i</sub> = 74 nF Temperature Range = -20 °C to +70 °C Max. cable length = 45 m		N/A
Electromagnetic Compatibility:	Emissions: EN61000-6-3; Immunity: EN61000-6-2; Certification: CE Marked		
Insulation Resistance:	> 100 MΩ @ 50 VDC		
Response time 10-90 %:	1 mS		
Wetted Parts:	Nickel plated brass, silicone tubing, silicon diaphragm, glass filled polyamide		
Pressure Media:	Non-corrosive media such as non-ionic fluids, air and dry gases		
Pressure Connection:	4 mm I.D. hose (other options available)		
Electrical Connection:	Screw terminals for conductor sizes 0.2-2 mm <sup>2</sup> are located beneath the enclosure lid. Cable entry is via IP66 cable gland with compression seal for cable sizes 7-10.5 mm		
Net. Weight (Kg):	0.3 Kg		

Figure 41 Datasheet - Protran PR3202

## B.6 Orifice plate $\beta = 0.6401$


Data sheet for		NO	BY	DATE	SHEET: 1	OF 1
<b>FLOW ELEMENT</b>					SPEC#:	REV: 01
					JOB # : <b>NTNU</b>	
					P.O. : <b>NTNU</b>	
					DATE : <b>14.04.2008</b>	CHK:
					BY : <b>LKS</b>	APR:
Tag. No. :	<b>FE-003-Tilbud</b>	Eq./Line No. :				
Service :		Flowsheet :				
Manuf. :	<b>AUTEK</b>	Model No. :	<b>FEOR-010</b>			
<b>ELEMENT DATA</b>	Element Type :	<b>Orifice Plate-Standard</b>				
	Press. Tap Loc. / Type :	<b>Upstream / Corner</b>				
	Element Material :	<b>304 SS</b>				
	Beta Ratio(d/D) :	<b>0,6401</b>				
	Element Bore :	<b>160,0180</b>	mm			
	Thickness :	<b>0,0000</b>	mm			
<b>SIZING CRITERIA</b>	Sizing Mode :	<b>Exact Bore</b>				
	Reference :	<b>ISO 5167-2003</b>				
<b>PIPING DATA</b>	Flange :	<b>150#</b>	/ RF			
	Pipe Size & SCH :					
	Pipe I.D. :	<b>250,0000</b>	mm			
	Flange Material :	<b>304 SS</b>				
	Pipe Material :	<b>316 SS</b>				
<b>COEFFICIENTS</b>	Discharge Coeff.(C) :	<b>0,605</b>	User Factor (Fuser) :	<b>1,000</b>		
	Gas Expan. Coeff.(Y1) :	<b>0,922</b>	Murdock Wet Gas Factor (Fx) :			
	Reynolds No.(Pipe) :	<b>843052,92</b>	Velocity of Approach Factor (Ev) :	<b>1,096</b>		
	Reynolds No.(Bore) :	<b>1317122,15</b>	Reynolds No.(Pipe - Normal) :	<b>736110</b>		
<b>PROCESS DATA</b>	Base	Maximum Flow	Normal Flow	Property Method		
Flow Rate :		<b>3,00</b>		kg/sec		
Diff. Pressure :		<b>250,00</b>		millibar		
Pressure Loss :		<b>146,09</b>		millibar		
Static Pressure :		<b>1,00</b>		Bar		
Base Pressure :						
Temperature :		<b>20,00</b>		DEG C		
Density :		<b>1,19</b>		kg/m3		
Spec. Gravity :				Redlich-Kwong		
Z-Compressibility Factor :		<b>0,999</b>				
Viscosity :		<b>0,02</b>		cP		
k-Factor (Cp/Cv) :		<b>1,4016</b>		User Input		
Fluid Name / Fluid State :	<b>Air</b>			Redlich-Kwong Equation		
Liquid Density :						
Gas Quality :						
<b>UNCERTAINTY DATA</b>	Uncertainty in Flow Rate :					
	in Discharge Coeff. :	<b>±0,57%</b>				
	in Expansion Factor :	<b>±0,62%</b>				
	in Primary Diameter :	<b>±0,05%</b>				
	in Pipe Diameter :	<b>±0,30%</b>				
	in Density :					
	in Pressure :					
Notes :						
						 WWW.AUTEK.NO

This report created by Flowel 4.0

PRINTED:22.08.2008 09:48:09

Figure 42 Datasheet - Orifice plate  $\beta = 0.6401$

## B.7 Orifice plate $\beta = 0.4018$

Data sheet for		NO	BY	DATE	SHEET: 1 OF 1	
<b>FLOW ELEMENT</b>					SPEC#:	REV: 01
					JOB # : NTNU	
					P.O. : NTNU	
					DATE : 14.04.2008	CHK:
					BY : LKS	APR:
Tag. No. : FE-003-Tilbud		Eq./Line No. :				
Service :		Flowsheet :				
Manuf. : AUTEK		Model No. : FEOR-010				
<b>ELEMENT DATA</b>		Element Type : Orifice Plate-Standard				
		Press. Tap Loc. / Type : Upstream / Corner				
		Element Material : 304 SS				
		Beta Ratio(d/D) : 0,4018				
		Element Bore : 100,4458 mm				
		Thickness : 0,0000 mm				
<b>SIZING CRITERIA</b>		Sizing Mode : Exact Differential				
		Reference : ISO 5167-2003				
<b>PIPING DATA</b>		Flange : 150# / RF				
		Pipe Size & SCH :				
		Pipe I.D. : 250,0000 mm				
		Flange Material : 304 SS				
		Pipe Material : 316 SS				
<b>COEFFICIENTS</b>		Discharge Coeff.(C) : 0,603				
		Gas Expan. Coeff.(Y1) : 0,988				
		Reynolds No.(Pipe) : 140508,82				
		Reynolds No.(Bore) : 349712,89				
		User Factor (Fuser) : 1,000				
		Murdock Wet Gas Factor (Fx) :				
		Velocity of Approach Factor (Ev) : 1,013				
		Reynolds No.(Pipe - Normal) : 736110				
<b>PROCESS DATA</b>		Base	Maximum Flow	Normal Flow	Property Method	
Flow Rate :		0,50			kg/sec	
Diff. Pressure :		45,98			millibar	
Pressure Loss :		37,76			millibar	
Static Pressure :		1,00			Bar	
Base Pressure :						
Temperature :		20,00			DEG C	
Density :		1,19			kg/m3	Redlich-Kwong
Spec. Gravity :						
Z-Compressibility Factor :		0,999				
Viscosity :		0,02			cP	User Input
k-Factor (Cp/Cv) :		1,4016				Redlich-Kwong Equation
Fluid Name / Fluid State :	Air				Gas	
Liquid Density :						
Gas Quality :						
<b>UNCERTAINTY DATA</b>		Uncertainty in Flow Rate :				
		in Discharge Coeff. : $\pm 0,50\%$				
		in Expansion Factor : $\pm 0,11\%$				
		in Primary Diameter : $\pm 0,05\%$				
		in Pipe Diameter : $\pm 0,30\%$				
		in Density :				
		in Pressure :				
Notes :						
					 WWW.AUTEK.NO	

This report created by Flowel 4.0

PRINTED:22.08.2008 08:42:51

Figure 43 Datasheet - Orifice plate  $\beta = 0.4018$



## C Sensitivity coefficients

$$\frac{\partial \rho}{\partial p} = \frac{1}{RT} \quad (1)$$

$$\frac{\partial \rho}{\partial T} = -\frac{p}{RT^2} \quad (2)$$

$$\frac{\partial \varepsilon}{\partial \beta} = 7.44(0.138\beta^3 + \beta^7) \left( \left(1 - \frac{\Delta p}{p_1}\right)^{1/k} - 1 \right) \quad (3)$$

$$\frac{\partial \varepsilon}{\partial p_1} = \frac{(0.351 + 0.256\beta^4 + 0.93\beta^8)\Delta p \left(1 - \frac{\Delta p}{p_1}\right)^{1/k}}{kp_1(p_1 - \Delta p)} \quad (4)$$

$$\frac{\partial \varepsilon}{\partial \Delta p} = -\frac{(0.351 + 0.256\beta^4 + 0.93\beta^8) \left(1 - \frac{\Delta p}{p_1}\right)^{1/k-1}}{kp_1} \quad (5)$$

## D Uncertainty analysis

### D.1 LD300 D-1

The same procedure is used as in chapter 5 in terms of stability and temperature effect. With an intended span equal 50 mbar and URL equal 50 mbar. The datasheet is listed in Appendix B.4.

**1. Pressure transmitter uncertainty,  $u(\Delta\hat{P}_{transmitter})$ :**

$$u(\Delta\hat{P}_{Transmitter}) = \frac{0.00075 \cdot 50}{2} = 0.019 \text{ mbar}$$

**2. Stability,  $u(\Delta\hat{P}_{Stability})$ :**

$$u(\Delta\hat{P}_{Stability}) = \frac{[(0.002 \cdot 50)]}{2} = 0.050 \text{ mbar}$$

**3. Temperature effect,  $u(\Delta\hat{P}_{Temperature\ effect})$ :**

$$u(\Delta\hat{P}_{Temperature\ effect}) = \frac{[(0.0008 \cdot 50 + 0.0005 \cdot 50) \cdot \frac{5}{20}]}{2} = 0.008 \text{ mbar}$$

**Table 16 Uncertainty budget - DP transmitter LD300 D-1**

Source	Input uncertainty				Combined uncertainty		
	Expanded uncertainty	Confidence level	Con. factor $k$	Standard uncertainty	Sens. coeff.	Variance	
Transmitter uncertainty	0.038 mbar	95 %	2	0.019 mbar	1	$3.52 \cdot 10^{-4} \text{ (mbar)}^2$	
Stability	0.100 mbar	95 %	2	0.050 mbar	1	$0.003 \text{ (mbar)}^2$	
Temperature effect	0.016 mbar	95 %	2	0.008 mbar	1	$6.60 \cdot 10^{-5} \text{ (mbar)}^2$	
Static pressure effects	Eliminated when installed	95 %	2	-	1	-	
Sum of variance					$u_c^2(\Delta\hat{P})$		0.003 mbar
Combined standard uncertainty					$u_c(\Delta\hat{P})$		0.055 mbar
Expanded uncertainty (95 % confidence level, $k = 2$ )					$U(\Delta\hat{P})$		0.110 mbar
Operating DP					$\Delta P$		X
Relative expanded uncertainty (95 % confidence level)					$U(\Delta P)/\Delta P$		0.110 mbar/X

## D.2 LD300 D-0

The same procedure is used as in chapter 5 in terms of stability and temperature effect. With an intended span equal 10 mbar and URL equal 10 mbar. The datasheet is listed in Appendix B.4.

### 1. Pressure transmitter uncertainty, $u(\Delta\hat{P}_{transmitter})$ :

$$u(\Delta\hat{P}_{Transmitter}) = \frac{0.001 \cdot 10}{2} = 0.005 \text{ mbar}$$

### 2. Stability, $u(\Delta\hat{P}_{Stability})$ :

$$u(\Delta\hat{P}_{Stability}) = \frac{[(0.002 \cdot 10)]}{2} = 0.010 \text{ mbar}$$

### 3. Temperature effect, $u(\Delta\hat{P}_{Temperature\ effect})$ :

$$u(\Delta\hat{P}_{Temperature\ effect}) = \frac{[(0.0015 \cdot 10 + 0.0005 \cdot 10) \cdot \frac{5}{20}]}{2} = 0.003 \text{ mbar}$$

Table 17 Uncertainty budget - DP transmitter LD300 D-0

Source	Input uncertainty				Combined uncertainty	
	Expanded uncertainty	Confidence level	Con. factor $k$	Standard uncertainty	Sens. coeff.	Variance
Transmitter uncertainty	0.010 mbar	95 %	2	0.005 mbar	1	$2.50 \cdot 10^{-5} \text{ (mbar)}^2$
Stability	0.020 mbar	95 %	2	0.010 mbar	1	$1.00 \cdot 10^{-4} \text{ (mbar)}^2$
Temperature effect	0.005 mbar	95 %	2	0.003 mbar	1	$6.25 \cdot 10^{-6} \text{ (mbar)}^2$
Static pressure effects	Eliminated when installed	-	2	-	1	-
Sum of variance						$1.31 \cdot 10^{-4} \text{ mbar}$
Combined standard uncertainty						0.012 mbar
Expanded uncertainty (95 % confidence level, $k = 2$ )						0.024 mbar
Operating DP						X
Relative expanded uncertainty (95 % confidence level)						0.024 mbar/X

### D.3 Protran PR3202

With an intended full scale (FS) of 50 mbar. The datasheet is listed in Appendix B.5.

**1. Pressure transmitter uncertainty,  $u(\Delta\hat{P}_{transmitter})$ :**

$$u(\hat{P}_{Transmitter}) = \frac{0.003 \cdot 50}{2} = 0.075 \text{ mbar}$$

**2. Temperature effect,  $u(\Delta\hat{P}_{Temperature\ effect})$ :**

$$u(\hat{P}_{Temperature\ effect}) = \frac{0.0004 \cdot 50 \cdot 5}{2} = 0.05 \text{ mbar}$$

**Table 18 Uncertainty budget - DP transmitter Protran PR3202**

Source	Input uncertainty				Combined uncertainty	
	Expanded uncertainty	Confidence level	Con. factor $k$	Standard uncertainty	Sens. coeff.	Variance
Transmitter uncertainty	0.150 mbar	95 %	2	0.075 mbar	1	0.005 (mbar) <sup>2</sup>
Temperature effect	0.100 mbar	95 %	2	0.050 mbar	-	0.003 (mbar) <sup>2</sup>
Zero offset and span tolerance	Eliminated when installed	95 %	2	-	1	-
Sum of variance						0.008 mbar
Combined standard uncertainty						0.090 mbar
Expanded uncertainty (95 % confidence level, $k = 2$ )						0.180 mbar
Operating DP						X
Relative expanded uncertainty (95 % confidence level)						0.180 mbar/X

